# Synopsis of thesis entitled

# Inhibition of fungal biodeterioration of construction materials using low and high ionizing radiation

**SUBMITTED FOR**

**THE DEGREE OF DOCTOR OF PHILOSOPHY**

**(ENGINEERING)**

**JADAVPUR UNIVERSITY**

**2023**


**By**

**ANIRBAN CHAUDHURI**

**Index No: D-7/ISLM/100/19**

**SCHOOL OF ENVIRONMENTAL STUDIES**

**JADAVPUR UNIVERSITY, KOLKATA-700032,**

**INDIA**

# Abstract

Fungal growth on concrete is a big challenge for building industries, real estate settlement in the modern world including India. The present study focuses on to prevent the invasive fungal damage in concrete using UVC and gamma radiation. To achieve this aim, concrete pieces were inoculated with pure cultures of *Aspergillus niger, Aspergillus tamarii, Aspergillus flavus* and *Penicillium oxalicum* which were isolated from 200 years old Tagore house at Jorasanko, north of Kolkata, West Bengal, India. The weight loss (%) of concrete piece, pH and color change of the fungal medium, oxalic acid production from HPLC (High Performance Liquid Chromatography) analysis, calcium leaching from micro EDXRF (Energy Dispersive X-ray Fluorescence Spectroscopy) study, SEM (Scanning Electron Microscope) images of fungal colonization on concrete surface after 30 days showed that *A. tamarii* imparted the maximum loss compared to other fungal species. A long term biodeterioration study of M40 and M20 graded concrete cube was subsequently performed with pure culture of *A. tamarii* to observe the changes in the concrete cube. After 180 days, the loss of weight and compressive strength of the infected concrete cubes (M40 and M20) compared to the control were 1.20 ± 0.01%, 2.22 ± 0.04%, 24.34 ± 0.16% and 25.17 ± 0.12% respectively. The fungal development and expansion of fungal hyphae into the interior of concrete cubes, which was deemed to be responsible for crack formation, which clearly visible in the stereo zoom microscope and SEM images. The micro EDXRF analysis further revealed that reduction in calcium mass for M40 and M20 graded concrete were 25.36 ± 0.05% and 15.68 ± 0.09% as well as absence of several spectral bands from FTIR (Fourier Transform Infrared Spectroscopy) study after 180 days which supported the *A. tamarii's* propensity for such deteriorating effect. Dose selection study was then performed for 30 days to find out the changes in properties in the *A. tamarii* infected concrete cube (M20) after exposure of UVC and gamma irradiation in radiation chamber. According to the concrete cube's physical, mechanical, and chemical properties, UVC (5 min) and gamma (0.5 KGy) radiation were required to prevent fungal biodeterioration without any deterioration of concrete cube caused by radiation. Radiosensitivity test was performed to select the most potent dose for complete inhibition of *A.tamarii*. The investigation reflected that *A. tamarii* was resistant after 5 min UVC and 0.5 KGy gamma exposures in radiation chamber but 20 min UVC and 1 KGy gamma radiation were needed for complete depletion of fungal population. Long term inhibition study was performed with M20 grade concrete for 180 days to observe the efficacy of the selected doses of radiation. Negligible weight losses (0.28 ±

0.09% and 0.72 ± 0.08%) were observed in UVC and gamma exposed infected concrete cubes as well as compressive strength of the cubes were improved compared to only infected samples. Strong stretching bands and greater calcium content (%) were also observed via the FTIR and micro EDXRF study in irradiated as well as infected cubes (66.43 ± 0.06% and 54.11 ± 0.07%) than the only infected ones. The usage of selected ultraviolet and gamma radiation doses demonstrated the effectiveness of minimising these prominent visible and chemical modifications of concrete materials against the growth of *A. tamarii.*

## Introduction

Concrete is an useful widely accepted composite man-made construction material, mainly constituted with cement, water, sand and stone chips. Concrete is widely used building material in the construction of different structures such as dams, weirs, houses, foundations, roads, bridges, sewers, pipes, culverts etc are various examples of civil engineering applications. However deterioration of concrete is an adverse phenomenon of down-gradation of cementitious materials to a lower vulnerable quality that reduce the life of material. When this deterioration is brought about by biological factors, it is termed as biodeterioration, which is an undesired negative change in the properties of a material due to the dominant activities of kind of living organisms (Rose 1981).

Fungi are chemoheterotrophic organisms that are common in subaerial and subsurface habitats. Autumn and summer are the prevailing seasons with the highest fungal levels in environment, while winter and spring have the lowest. *Aspergillus* sp., *Penicillium* sp., *Cladosporium* sp., and nonsporulating fungi which are the most prevalent cultivable airborne fungi inside throughout all seasons and regions (Reddy et al., 2017). Most of fungi present in indoors come from outdoor sources in normal houses and buildings (Nevalainen et al., 2015). Generally fungi enter a building through windows and doors, through outside air intakes of the ventilation, heating, and air conditioners, and contaminate building materials and other structural elements. Moreover, sick building syndrome (Sykes 1988) is a global phenomenon and a disease confirmed by the World Health Organization (Sarkhosh et al., 2021) predominantly by the active fungal ingress.

Now a day's mold growth in homes is one of the vital problems in the house construction industry. In most of the buildings, the main reason of mold growth is seepage. The cement constructed walls of the buildings with internal seepage either due to rains or leakages in washroom or air conditioning system which supports indoor fungal growth. In suitable

temperature and humidity for their growth, in form of fungal colony and degrade the properties of concrete. Concrete weathering, abrasion, deterioration, carbonation, corrosion, and chloride ion penetration are caused by physical, mechanical and chemical factors. This phenomenon shortens the concrete's lifespan and hiking the maintenance cost. The annual loss worldwide from fungal attacks on archives, apparel and construction materials are over Rs 2.7 lakh crores (US$40 billion) as stated by Allsopp (2011).

In the present investigation, fungal affected historical buildings are taken into consideration and field observations are done. After thoroughly examination, lots of mold in wood, concrete, marble and painting surfaces are physically observed. This study revealed that fungi present in this heritage building were *Aspergillus niger, Aspergillus tamarii, Aspergillus flavus and Penicillium oxalicum.* This finding motivated the researcher to carry out further research for exploring how the fungi biologically deteriorates the physical, mechanical, chemical and aesthetic properties of concrete. In this matter, no such integrated study has been carried out in detail in the past to identify the fungi, loss determination and prevention by some important physical radiological phenomenon to eradicate the problem. The present research is addressed for the reduction of such gap.

Most taxa in the kingdom fungi are known for their filamentous growth habit and special ability to develop by extending their hyphal tips. Moreover, filamentous fungi have strong, flexible cell walls that allow them to penetrate into concrete materials to seek and acquire nutrient resources. Indeed, filamentous fungi can colonise and grow in concrete structures under favourable conditions of temperature and moisture, provided they have access to enough nutrients, energy, and organic carbon sources. This can have a detrimental effect on the concrete's physical, mechanical, chemical, and aesthetic properties (Tong 2018). Gene of fungi or phylum of fungi responsible for such corrosion and identification needed for that. Furthermore, necessary methods and assessment for remediation of fungal affected materials is the present scope of study.

Ionizing and non-ionizing radiation have successfully been used in the recent past year to disinfect cultural heritage structures with the assistance of libraries and museum authorities (Bertrand et al., 2023). Additionally, a lot of materials can be irradiated at once. This technology does not harm the environment or leave any residue behind. Therefore, there is no risk to the environment or to conservators/restorers, museum curators and registrars, or operators of irradiation facilities.

The use of UVC and gamma radiation to prevent microbial contamination of concrete materials has only recently been described in few research studies (Borderie et al., 2012; Kontani et al., 2014). Radiation-related knowledge on the physical, mechanical, and chemical deterioration of concrete materials was thought to be scarce up till date. With this view point, the present studies has been undertaken to choose an acceptable UVC and gamma radiation exposure dose to prevent fungal biodeterioration of concrete with the least possible loss of the materials in its physical, mechanical, and chemical properties. On fungus inoculated on concrete, a growth environment extremely similar to that actually found on buildings, the effectiveness of the UVC and gamma exposure strategy to restrict the fungal biodeterioration for some time duration was also established. The outcome of the present investigation will be helpful for knowledge base research findings of deterioration of concrete materials due to fungal attack in indoor environment and to examine the physical, mechanical, chemical and aesthetic properties. These findings also support for standardization of some non-destructive method such as application of ultraviolet and gamma radiation for reduction of such fungal deterioration.

## Objectives of work

The objective of the present work is to explore and evaluate biodeterioration potential for concrete specimen due to invasion of some potent airborne fungi along with assessment of physico-chemical change of the infected concrete materials with radiation effect for resisting fungal effect.

## Materials and methods

### 1.1 Isolation of fungal species from ambient air

#### 1.1.1 Fungal sampling locations

The location of sampling sites were chosen at different places such as library, computer room, creche, cafeteria, beauty parlour salon and separately one outdoor (control) area located in Kolkata, India. The average humidity was kept as 66% and the temperature fluctuates between 22 and 27 °C.

#### 1.1.2 Preparation of agar plates

For the necessary culture of yeasts and moulds, both Rose Bengal Agar (RBA) medium and Potato Dextrose Agar (PDA) medium were both used. After carefully maintaining the pH for

both medium (7.2 and 5.6), the ingredients were properly mixed in distilled water before being autoclaved at 15 pounds per square inch pressure for 15 min. 20 mL of medium was then added to each sterile petri plate, and left until it hardened.

### 1.1.3 Sampling procedure and fungal load determination

The fungal spores were collected with Two-Stage Viable Andersen Cascade Impactor. After reaching the chosen location, the impactor was placed at a relatively undisturbed location inside the room. Then, in a sequential manner, each set of medium plates was take out and put to the second stage, with its corresponding matching pair in the first stage. For both of these medium, Andersen sampler was run for 15 min at each sampling sites. At last the plates were kept in an incubator for 7 days at 27 °C. Colony growth was visible on the plates after 7 days in the incubator. After staining with lacto phenol cotton blue, each colony was examined with a compound microscope at 100× magnifications. The following equation was used to determine the amount of fungi per cubic metre of air:

$$\textbf{Colony} - \textbf{forming unit} = \frac{\mathbf{1000P}}{\mathbf{RT}}\,\mathbf{CFU/m^3}$$

Where P = number of counted colonies on the sample plate after correction using positive hole conversion table (Andersen 1958), T = time (15 min), R = rate of air sampling (14 L/minute).

## 1.2 Isolation of fungal species from damp walls

### 1.2.1 Location of fungal sampling

The subject area for our current study was the Tagore residence in Jorasanko, Kolkata, India. Our study site, which was 200 years old and 6 m above sea level, was close to the Hooghly River. The temperature varies between 24 and 38 $^0$C in the summer and between 12-27 $^0$C in the winter. Around 1582 mm of rain falls annually on average between June and September.

### 1.2.2 Procedure of sampling

Fungi was isolated from three distinct locations of the fungal infected surface (4 cm$^2$ area) of the wall of Tagore's house by rubbing a sterilized cotton swab at a height of 2.5 m from the ground. Subsequently, the cotton swab was dipped in 1 mL of sterile Czapek Dox broth and then inoculated into the Czapek Dox Agar plates. For consequently seven days, the plates

were incubated at 27 °C. Thereafter slides were prepared for each colony and observed under light microscope.

### 1.3 Selection of predominant fungi for adverse effects

This study was performed to select most potent fungal strain involved in biodeterioration of concrete. Concrete pieces (250 $mm^2$ surface area) were used for this study.

#### 1.3.1 Preparation of fungal spore suspension

In a conical flask, semi-synthetic fungal (Czapek Dox Agar) medium was prepared. The medium (pH 7.3 ± 0.2) was then sterilised for 15 min at 121 $^0$C and 1.0546 kg/$cm^2$ pressure. After that, the sterile medium in the conical flask was tilted at an angle of $45^0$ and left to solidify. With the aid of a sterilised inoculating loop, a loop of fungal culture was collected and streaked over the agar surface in a conical flask. The agar slants were then kept in an incubator at 27 $^0$C. The fungal spores (1.8 x $10^5$ spores/ml) in the slants were combined with the autoclaved distilled water after the 7-day incubation period. Finally, fungal spore suspensions for each fungus species was filled into a sterilized conical flask and kept them ready for use.

#### 1.3.2 Experimental set up

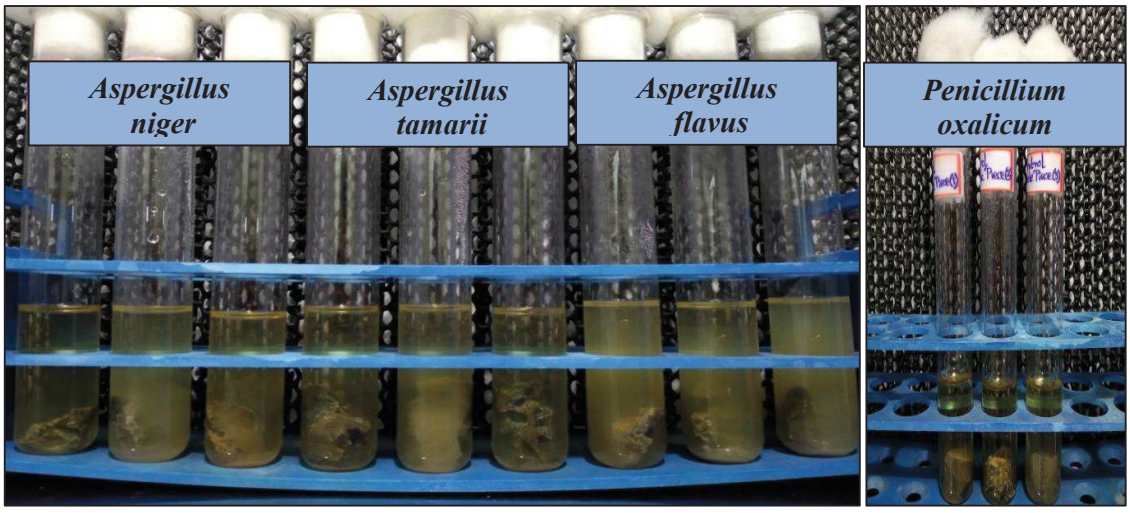


**Fig. 1** Setup of test tubes for selection of most potent fungus.

Each 70 ml test tube was filled with 20 mL of Czapek Dox medium. Next the sample concrete pieces chosen were dipped into the medium. Magnesium sulphate, potassium

chloride and ferrous sulphate were absent in the medium because these salts were already present in concrete samples. After that all the above test tubes were put in an autoclave for sterilization. After sterilization, the medium was cooled at ambient temperature (27 ± 5 °C). At last 2 mL of each fungal spore suspensions was added in that particular test tube with the help of 5 mL pipette in laminar airflow chamber. The entire set up (Fig. 1) was kept in an incubator for 30 days at a temperature of 27 °C and a relative humidity of 75%.

### 1.4 Biodeterioration study

#### 1.4.1 Experimental set up of concrete cubes

**Fig. 2** Experimental set up for deterioration test of: a) M40 grade concrete (10 cm x 10 cm x 10 cm); b) M20 grade concrete (5 cm x 5 cm x 5 cm) cubes.

Airtight plastic containers [(38 cm × 26 cm × 18 cm) and (30 cm × 20 cm × 15 cm)] were used for biodeterioration test. M40 (10 cm x 10 cm x 10 cm) and M20 (5 cm x 5 cm x 5 cm) graded concrete cubes were kept in the containers containing sterilized (121 °C temperature at 15 psi pressure for 15 min) Czapek Dox medium (pH 7.3 ± 0.2) and injected with the spore suspension of most potent fungus (*A. tamarii*) (Fig. 2). Additionally, a control was run for 180 days in sterile medium. At a temperature of 27 $^0$C and a relative humidity of 75%, the full set was incubated. In intervals of 60 days, it was observed for 180 days.

### 1.5 Selection of radiation dose

#### 1.5.1 Radiosensitivity test of *A. tamarii*

The fungus that was isolated from deteriorated walls of the Tagore's residence was used to calculate the necessary dose needed to inactivate fungus on axenic cultures. The most

dominant fungus (*A. tamarii*) from the preliminary study was inoculated on Petri dishes with Czapek Dox Agar and incubated at 27 $^{0}$C for 2 days. Following incubation period the cultures were exposed to a $^{60}$Co gamma source for irradiation at 20 $^{0}$C with exposure doses of 0.5, 0.75, 1.0 KGy (1.27 KGy/h) and UVC exposure of 5, 10, 15, 20 min respectively. The UVC light of intensity 625 μw/cm² and 254 nm peak was used in the current investigation. The distance between light and applied surface of plate was 15 cm. After irradiation the plates were incubated at 27 $^{0}$C for 7 days. The controls were grown on Czapek Dox Agar and kept under the same conditions as the treated fungus. On the first, fourth and seventh days after irradiation, the colony diameter was measured to check for fungal development in comparison to the colony diameter measured just before irradiation and to the controls. All these biological assays were done in triplicate.

### 1.5.2 Radiation on concrete cubes

#### 1.5.2.1 Arrangement of concrete cubes

Airtight sterilized plastic boxes (24 cm × 19 cm × 9 cm) and 5 cm × 5 cm × 5 cm concrete cube (M20) were both used for current study. In separate plastic containers, the formed concrete cubes were placed in various arrangements that were observed after 30 days. The arrangements included a biodeterioration set (cubes were infected with *A. tamarii*), inhibition sets (cubes were inoculated with same fungus and exposed to multiple doses of ultraviolet and gamma radiation), a control set (non-infected and non-irradiated), and multiple control sets (cubes were irradiated with multiple doses of both radiation).

#### 1.5.2.2 Experimental set up for radiation application

Using a paint brush, spore suspension of *A. tamarii* was applied on the concrete cubes (biodeterioration and inhibition) within polyethylene boxes before adding autoclaved Czapek Dox medium (1/10$^{th}$ height of cube) in laminar air flow cabinet. The control sample i.e. non-infected and non-irradiated sample was run in sterile Czapek Dox medium. Then an incubator was used to keep the boxes for control (non-infected and non-irradiated) and biodeterioration (infected) at a constant temperature of about 27 ± 2 $^{0}$C and a relative humidity of 50 ± 2% for 7 days. The inhibition sets before irradiation was also maintained at the same temperature and humidity level in order to see the fungal growth on the concrete cube's surface visually. At the 8$^{th}$ day, the inhibition (infected and irradiated) cube samples were exposed to UVC light for 5, 10, 15 and 20 mins on the irradiation chamber [Fig. 3(a)].

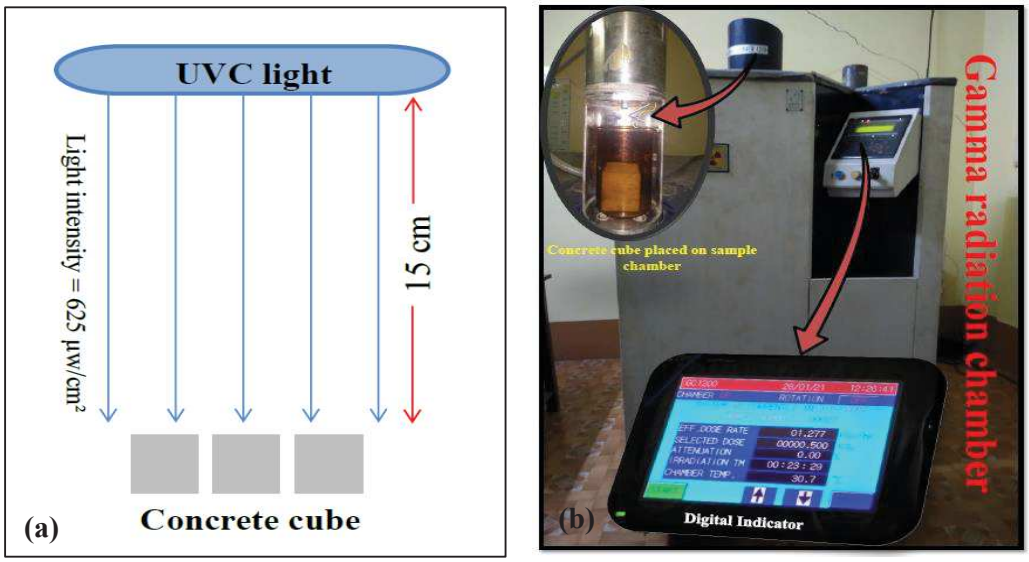


**Fig. 3** Concrete cubes were irradiated with: a) UVC; b) Gamma radiation.

For gamma radiation, inhibition concrete cubes were subjected to a $^{60}$Co gamma source for irradiation [Fig. 3(b)] at 20 $^{0}$C with exposure doses of 0.5, 0.75 and 1.0 KGy. The same dosages of UV and gamma radiation were also applied to the control cubes (irradiated). Finally, the control (irradiated) and inhibition (infected and irradiated) concrete cubes were put into the cleaned plastic boxes which contained the same medium (sterile). Both setups were incubated at the same humidity and temperature for thirty days of retention time.

### 1.6 Inhibition study with selected radiation dose

#### 1.6.1 Arrangements of concrete cubes

The study was conducted in airtight plastic boxes measuring 24 cm × 19 cm × 9 cm were also employed. Surface sterilizing was used to clean the box. Both infected sets (cubes were infected with *A. tamarii* and exposed to a selected dose of ultraviolet and gamma radiation from previous study) and multiple control sets (cubes were exposed to a preselected dose of ultraviolet and gamma radiation) were included in the arrangements.

#### 1.6.2 Experimental set up

The M20 graded concrete cubes (5 cm × 5 cm × 5 cm) for infected sets were initially coated with a spore suspension of same fungus using a paintbrush inside a plastic container. After that, sterile Czapek Dox medium was added into the plastic box. The box was then placed

into the incubator at 27 $^{0}$C. After 7 days of incubation period, concrete cubes (infected) were exposed with the selected dose (from dose selection study) of UV and gamma radiation. The control cubes were also irradiated with the same dose of radiations. After cleaning the boxes and addition of fresh sterile Czapek Dox medium (pH 7.3±0.2), the exposed concrete cubes (control and infected) were finally placed inside for 180 days at 27 $^{0}$C temperature and 75% relative humidity.

### 1.7 Characterization of concrete cube

HPLC was performed for the detection of organic acids that may damage concrete cubes and also present in the fungal medium. To analyse the surfaces and internal features of concrete cube, both stereo zoom microscope and scanning electron microscope were utilised.

Mechanical properties were assessed by measuring the concrete cubes compressive strength with the compression testing machine. By weighing the initial and final weights of each cube, the weight variation (%) was calculated. Concrete cubes were broken down into chips and powder from the infected portion of the cubes. Concrete powdered samples were utilised to show changes in the functional groups by using an FTIR spectrometer, and concrete chips were used for the study of trace elements by micro EDXRF.

### 1.8 Statistical analysis

For each of the specimen sample, all experiments were performed in triplicate and standard deviation has been shown as error bars and values in results and discussion section. In order to compare the differences between the mean values of control (non-infected and non-irradiated) and biodeteriorated (infected) concrete specimens as well as control (irradiated) and inhibition (infected and irradiated) specimens, the Student's *t*-test was also carried out for all experiments. The asterisks above columns in bar graphs and line graphs present the p-value: $^{*}$, $p < 0.05$; $^{**}$, $p < 0.01$; $^{***}$, $p < 0.001$.

# Results and discussions

## 2.1 Selection of predominant fungus for adverse effect

### 2.1.1 Identification of micro-fungi isolated from ambient air

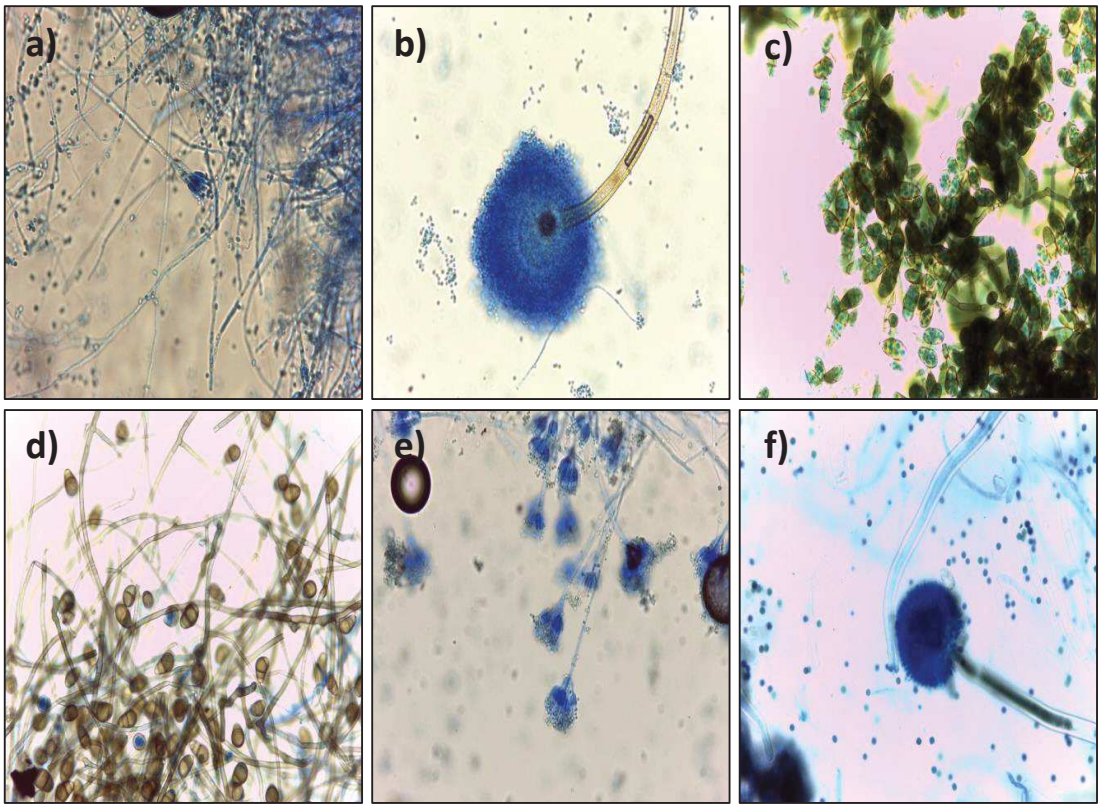


**Fig. 4** Compound microscope images (100× magnification) of: a) *Penicillium* sp. from library; b) *Aspergillus* sp. from library; c) *Diasporium* sp. from computer room; d) *Alternaria* sp. from creche; e) *Penicillium* sp. from cafeteria; f) *Aspergillus* sp. from salon.

*Aspergillus* sp., *Penicillium* sp., *Paecilomyces* sp. and *Rhizopus* sp. were the dominating genera in library [Fig. 5(a)]. *Aspergillus* sp., *Penicillium* sp., *Paecilomyces* sp., *Cladosporium* sp., *Curvularia* sp., *Alternaria* sp. and *Diasporium* sp. were found in computer room [Fig. 5(b)]. Two common fungal species i.e. *Aspergillus* sp. and *Penicillium* sp. were also identified from the indoor air of creche, cafeteria and salon [Fig. 5(c), Fig. 5(d) and Fig. 5(e)]. Aquino et al., (2013) discovered fungal contamination in the dust taken from the cafeteria, which is in contrary to the present observations. Moreover, *Alternaria* sp. and *Curvularia* sp. were also found in the air sampled from creche and salon.

### 2.1.1.1 Diversity and density of airborne micro-fungi

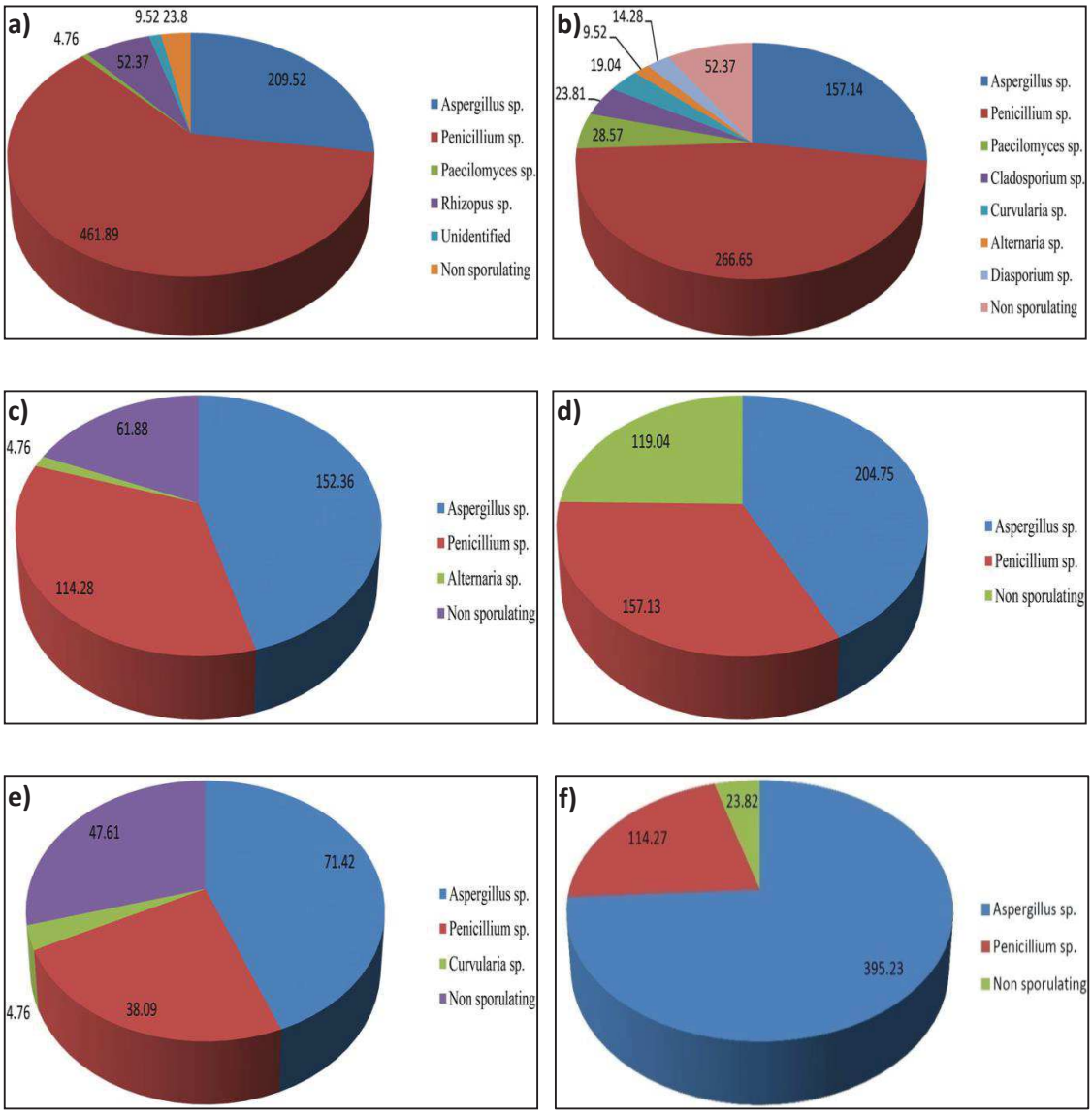


**Fig. 5** Density (CFU/m$^3$) of microflora in: a) library; b) computer room; c) creche; d) cafeteria; e) salon; f) outdoor.

In the air sampled from library, *Penicillium* sp. was the most abundant species (461.89 CFU/m$^3$), followed by *Aspergillus* sp. (209.52 CFU/m$^3$) and *Rhizopus* sp. (52.37 CFU/m$^3$) [Fig. 5(a)]. The similar pattern was seen in the air taken from a salon [Fig. 5(e)], where *Aspergillus* sp. (71.42 CFU/m$^3$) and *Penicillium* sp. (38.09 CFU/m$^3$) were the two most dominating genera. An earlier study of this kind was conducted in 257 saloons in the four selected areas of Ibadan, the capital of Oyo state, Nigeria which revealed that the most prevalent genera was *Aspergillus* sp. and *Penicillium* sp. followed by *Fusarium* sp. and

*Mucor* sp. (Sarah and Ee 2017). The highest percentage of culturable airborne fungi in outdoor environment [Fig. 5(f)] during monsoon season was found for *Aspergillus* sp. (395.23 CFU/$m^3$) followed by *Penicillium* sp. (114.27 CFU/$m^3$).

### 2.1.2 Identification of micro-fungi isolated from damp walls

After microscopic observation, the highest number of colony in this heritage building was found for *Aspergillus* sp. followed by *Penicillium* sp. The four fungal strains i.e. *Aspergillus niger, Aspergillus tamarii, Aspergillus flavus* and *Penicillium oxalicum* (Fig. 6) were identified from Tagore's house. *Aspergillus* sp. followed by *Penicillium* sp., *Alternaria* sp. was the most encountered species as reported by Skora et al., (2015).

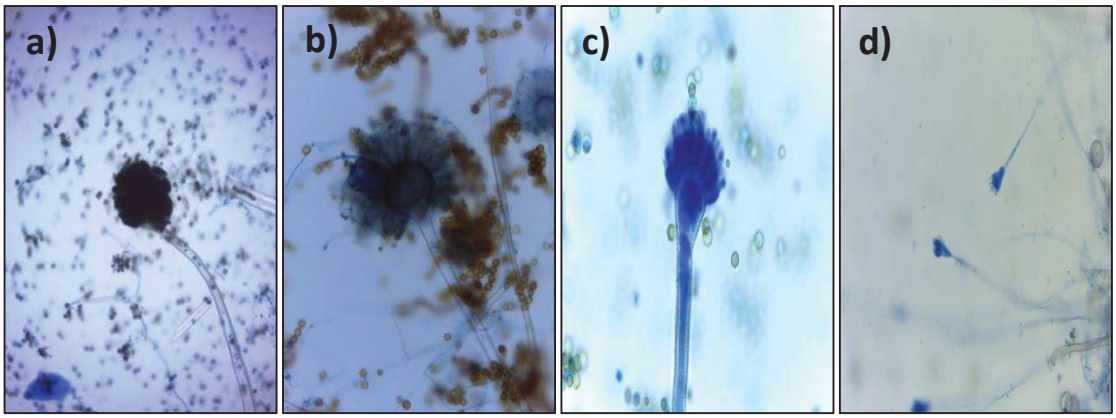


**Fig. 6** Compound microscope images (100× magnification) of: a) *Aspergillus niger*; b) *Aspergillus tamarii*; c) *Aspergillus flavus*; d) *Penicillium oxalicum.*

### 2.1.3 Selection of most adverse fungus for present study

#### 2.1.3.1 Loss of weight

Concrete pieces infected with *A. niger*, *A. tamarii*, *A. flavus* and *P. oxalicum* showed weight losses of 1.89 ± 0.08%, 2.84 ± 0.06%, 2.57 ± 0.08% and 2.45 ± 0.02% respectively and statistically significant ($p < 0.05$) compared to the control after 30 days of incubation period (Table 1). So, according to the percentage weight loss it was observed that *A. tamarii* attributed maximum deterioration for concrete. Similar observation of reduction in weight of concrete after fungal infection as reported by Gu et al., (1998).

**Table 1** Weight loss percentage of concrete pieces (n = 3) after 30 days of incubation.

| | Weight Loss (%) | Average loss (%) | Standard deviation (%) |
|---|---|---|---|
| Control | 0<br>0<br>0 | 0 | 0 |
| *Aspergillus niger* | 1.95<br>1.92<br>1.80 | 1.89 | 0.08 |
| *Aspergillus tamarii* | 2.78<br>2.90<br>2.86 | 2.84 | 0.06 |
| *Aspergillus flavus* | 2.60<br>2.63<br>2.47 | 2.57 | 0.08 |
| *Penicillium oxalicum* | 2.46<br>2.45<br>2.42 | 2.45 | 0.02 |

### 2.1.3.2 Organic acid analysis

**Table 2** Organic acids released by fungi that are involved in biodeterioration of concrete.

| **Fungal taxa** | **Organic acids** |
|---|---|
| *Aspergillus niger* | Oxalic acid, malic acid |
| *Aspergillus tamarii* | Oxalic acid, malic acid |
| *Aspergillus flavus* | Oxalic acid, malic acid, fumaric acid |
| *Penicillium oxalicum* | Oxalic acid |

The composition of organic acids in the liquid medium of *A. niger*, *A. tamarii, A. flavus and P. oxalicum* were also analysed. The results demonstrated that after 30 days of incubation the fungal medium contained oxalic acid, malic acid and fumaric acid respectively (Table 2).

Moreover, the majority of fungi like *Aspergillus*, *Penicillium* and *Fusarium* excreted acetic, citric, oxalic, malic, lactic, fumaric, gluconic, propionic, itaconic and succinic acids which resulted in corrosion of the concrete structures (Liaud et al., 2014).

### 2.1.3.3 SEM observation

#### 2.1.3.3.1 Fungal growth

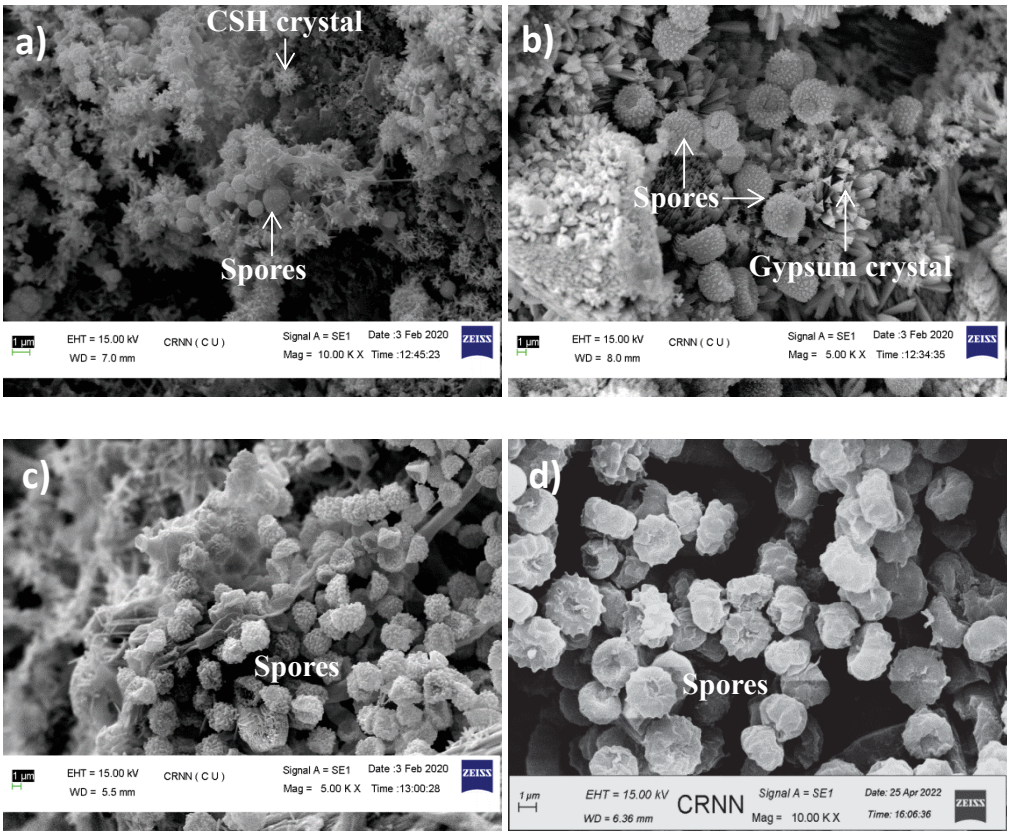


**Fig. 7** SEM images of: a) *A. niger*; b) *A. tamarii*; c) *A. flavus*; d) *P. oxalicum* exposed concrete samples after 30 days of incubation.

The control specimens showed no signs of fungi growing on them. After being exposed to *A. niger*, *A. tamarii*, *A. flavus*, and *P. oxalicum*, concrete samples were analysed under a scanning electron microscope to measure the degree of microbial colonisation. In the SEM pictures (Fig. 7), it was observed that spores grow quickly on concrete surfaces. Wiktor et al., (2009) demonstrated that fungal growth starts to develop after the first week of incubation on cement specimens confirmed by SEM observations.

### 2.1.3.3.2 Crack and ettringite formation

A few interesting results were obtained with the specimens inoculated with *A. tamarii*. SEM images [Fig. 8(a)] clearly evidenced that fractured crack surfaces of *A. tamarii* infected concrete samples were also observed by scanning electron microscope.

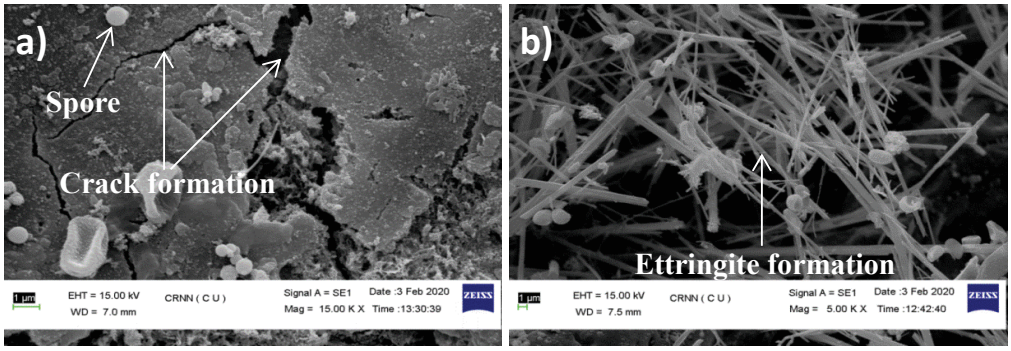


**Fig. 8** SEM images of: a) crack formation; b) ettringite formation on *A. tamarii* exposed concrete samples.

Amann et al., (1990) study studied earlier and found that the impact of microorganisms on concrete structures can be categorised based on how they affect the surfaces of the concrete and the matrices that produce cracking and encourage crack growth. Water and other salts percolating through these cracks initiate corrosion, and reduce the concrete's lifespan. SEM images of *A. tamarii* infected concrete samples depicted the formation of ettringite needles [Fig. 8(b)]. Fungi can secrete enzymes which interact with amino acids, that released by fungi, to generate thin needles of ettringite. Ettringite formation in hardened concrete has been reported that a potential property to lead for crack development and perhaps the reason for one of the mechanisms causing fungal influenced deterioration of concrete (Hanehara and Oyamada 2010).

### 2.1.3.4 Variation in elemental composition

The calcium percentage of *A. niger*, *A. tamarii*, *A. flavus* and *P. oxalicum* inoculated concrete were decreased ($p < 0.001$) to 48.58 ± 0.22%, 48.00 ± 0.19%, 49.37 ± 0.28% and 51.21 ± 0.30% respectively as compared to the control specimens (72.32 ± 0.42%). Also, it was shown earlier in the literature that fungi contributed for the leaching of calcium from the concrete cube (Sanchez-Silva et al., 2008). The calcium leaching rate increased over time, which resulted in a rise in silicon concentration (Fig. 9).

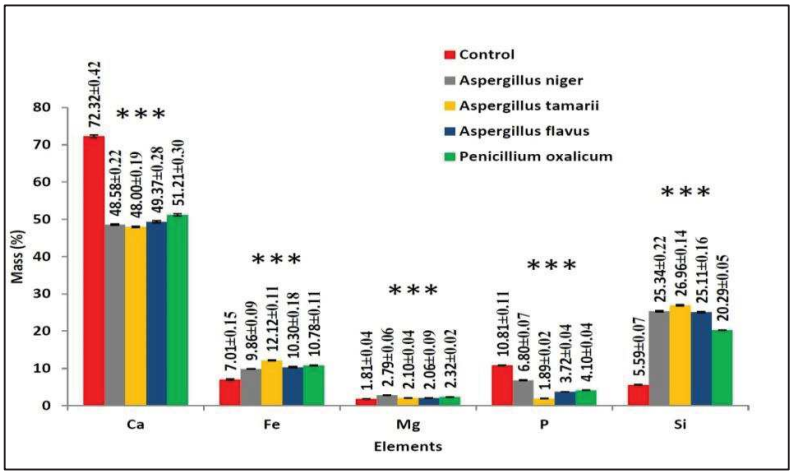


**Fig. 9** Mass fraction of different elements of concrete pieces (n = 3) after 30 days of incubation.

With the view point of weight loss, fungal growth observation, crack and ettringite formation, excretion of organic acids, change in elemental composition, it may be confirmed that *A. tamarii* enhanced maximum deterioration effect on concrete in different ways. Hence, all subsequent investigations in the present research were carried out with *A. tamarii* only as candidate microorganism.

## 2.2 Biodeterioration study

### 2.2.1 Weight loss

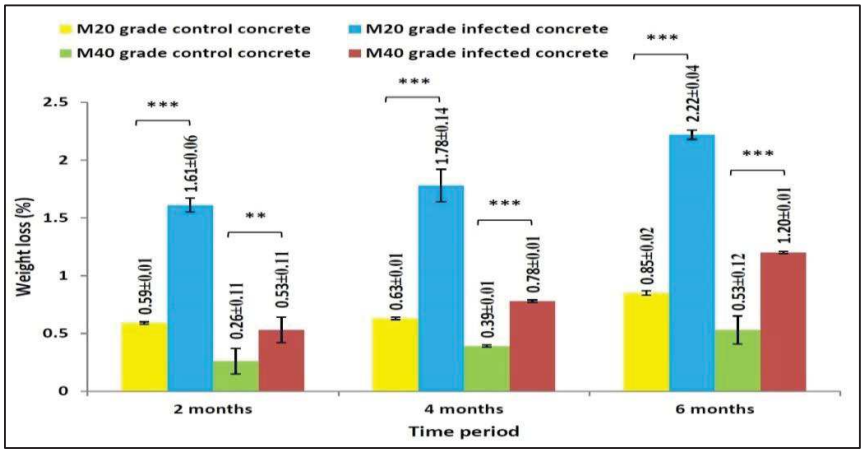


**Fig. 10** Weight loss of M20 grade and M40 grade control and infected concrete cubes (n = 3).

Experimental control concrete cubes exhibited weight losses of 0.59 ± 0.01%, 0.63 ± 0.01% and 0.85 ± 0.02% for M20 grade and 0.26 ± 0.11%, 0.39 ± 0.01% and 0.53 ± 0.12% for M40

grade concrete respectively after 6 months of incubation because Czapek Dox medium contains various compounds (chlorides or possibly nitrates) which accelerate calcium leaching. After incubation of 2, 4 and 6 months, 1.61 ± 0.06%, 1.78 ± 0.14% and 2.22 ± 0.04% weight losses have been observed for M20 graded infected concrete cubes whereas for M40 graded infected cubes 0.53 ± 0.11%, 0.78 ± 0.01% and 1.20 ± 0.01% weight losses respectively as shown in Fig. 10.

It was observed that the weight loss were increased in every time interval for M20 and M40 grade concrete cubes after infected with *A. tamarii* (Fig. 10). Interestingly the weight loss in M20 grade concrete cubes was more compared to the M40 grade cube in every interval. A similar observation were noticed earlier by Gu et al., (1998) using *Fusarium* sp. in concrete sample, where after 2 and 4 months, 1.5 and 6% weight losses were previewed. The weight loss of concrete cube indicates towards the deterioration of concrete.

### 2.2.2 Compressive strength loss

Compressive strength of the concrete cube decreased in every time period for fungal as well as control specimens. The compressive strength of the low and high graded control concrete cubes after 2, 4 and 6 months of studied period were 19.20 ± 0.14, 18.78 ± 0.09, 18.50 ± 0.08, 43.90 ± 0.08, 43.66 ± 0.05 and 43.28 ± 0.05 N/mm$^2$ respectively (Fig. 11). Also the average strength of *A. tamarii* infected M20 grade concrete cubes after 6 months was found to be decreased less (19.74 ± 0.11 N/mm$^2$ to 14.77 ± 0.06 N/mm$^2$) will be less compared to M40 grade concrete (44.00 ± 0.30 N/mm$^2$ to 33.29 ± 0.09 N/mm$^2$).

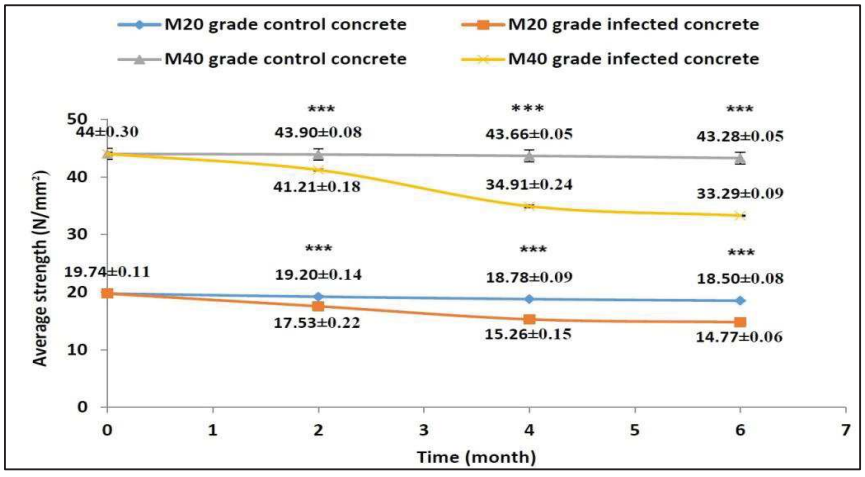


**Fig. 11** Compressive strength (N/mm$^2$) loss of M20 grade and M40 grade concrete cubes (n = 3) after exposure to *A. tamarii.*

Experimental data showed that the inoculation with *A. tamarii* accelerates the degradation process which reduced the cubes compressive strength (Fig. 11). The present study demonstrates that *A. tamarii* grew on the cube surface and penetrates with their hyphae as shown in SEM images (Fig. 15). This is likely one of the main causes of the compressive strength decreasing as incubation time increases (Aldosari et al., 2019).

### 2.2.3 Organic acid analysis

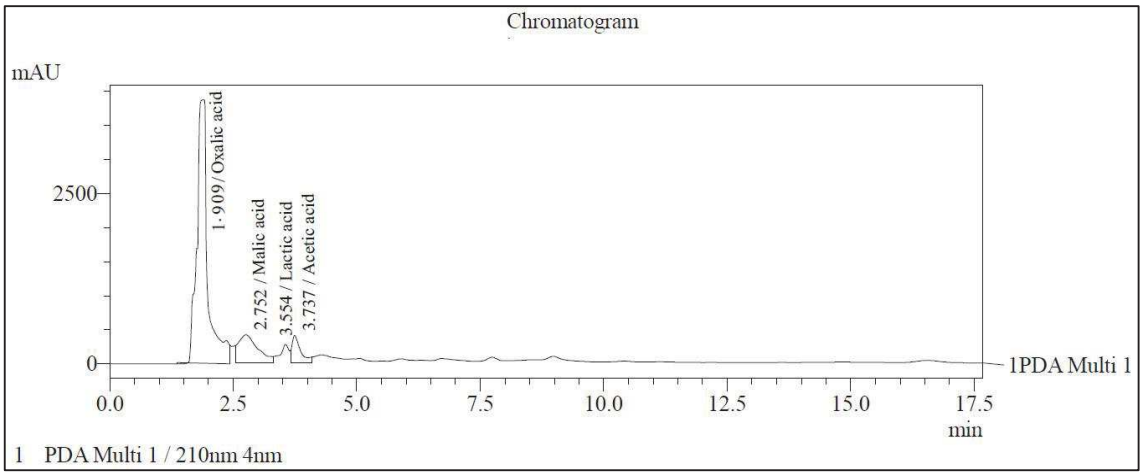


**Fig. 12** HPLC chromatograph of 6 months liquid medium of *A. tamarii* infected concrete cubes.

HPLC analysis for organic acid production after 6 months indicated four significant peaks identified as oxalic acid, malic acid, lactic acid and acetic acid (Fig. 12). Peak identification was established when sample peak retention times matched those of pure organic acid standards. It was also observed that oxalic acid dominates the acidity (from the fungus) due to its high concentration. Similar type of findings was also noticed in liquid culture medium of edible fungi and showed that oxalic acid was present in greater quantity followed by malic acid and citric acid (Yu et al., 2020). These acids could react with calcium hydroxide [$Ca(OH)_2$] in concrete and forms soluble salts such as calcium lactate [$Ca_3(C_6H_5O_7)_2$] and calcium acetate [$(CH_3COO)_2Ca$], which results in calcium leaching and insoluble salts i.e. calcium oxalate ($CaC_2O_4$) and calcium malate ($C_4H_4CaO_5$) causing expansion attack.

### 2.2.4 Variation in elemental composition

During the progress of time, the calcium content found to be decreased ($p < 0.001$). The percentage of calcium of M40 grade control concrete was 34.24 ± 0.06% and after 6 month

fungal infection it reached 25.36 ± 0.05% [Fig. 13(b)]. Similarly, calcium concentration in M20 grade control concrete was 69.63 ± 0.12% and after 2, 4 and 6 month fungal exposure interval it reached 43.63 ± 0.18%, 31.46 ± 0.22% and 15.68 ± 0.09% respectively [Fig. 13(a)].

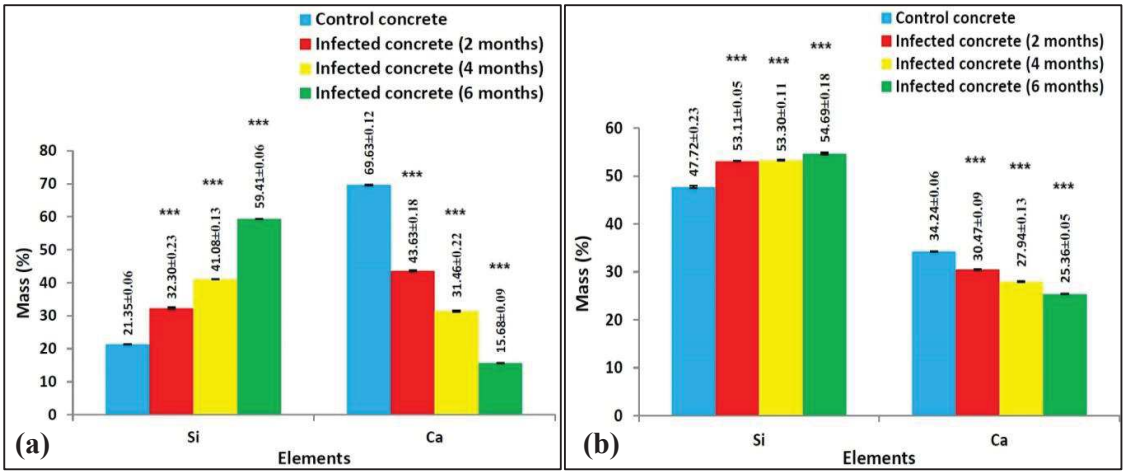


**Fig. 13** Mass fraction of silicon and calcium for control and *A. tamarii* infected: (a) M20 grade; (b) M40 grade concrete samples (n = 3).

Moreover, it has been also noted that fungal activity helps in the calcium leaching process from concrete cubes (Sanchez-Silva and Rosowsky 2008). Obviously, the rate of calcium leaching was less in M40 grade cube that can explain on the basis of compressive strength of the concrete cube and also porosity of the M20 grade concrete cubes for hyphae penetration to the substrate was more compared to the M40 graded cubes. Also, during a six-month study on deterioration, the concentration of silicon was increased (Fig. 13). As the calcium leaching rate accelerated over time, silicon content also increased ($p < 0.001$).

### 2.2.5 Variation in functional groups

The IR spectrum for control concrete showed the presence of portlandite [$Ca(OH)_2$] at 3640 $cm^{-1}$ (O-H stretching vibrations) which was vanished in *A. tamarii* infected samples. The transformations of portlandite occur during the leaching and carbonation of concrete. A strong symmetric stretching absorption band (C-O) of calcite at wavenumber 1400, 874 and 611 $cm^{-1}$ became medium in *A. tamarii* infected M40 grade concrete samples [Fig. 14(b)]. Also this band was absent in M20 grade concrete after 3 and 6 months fungal inoculation [Fig. 14(a)].

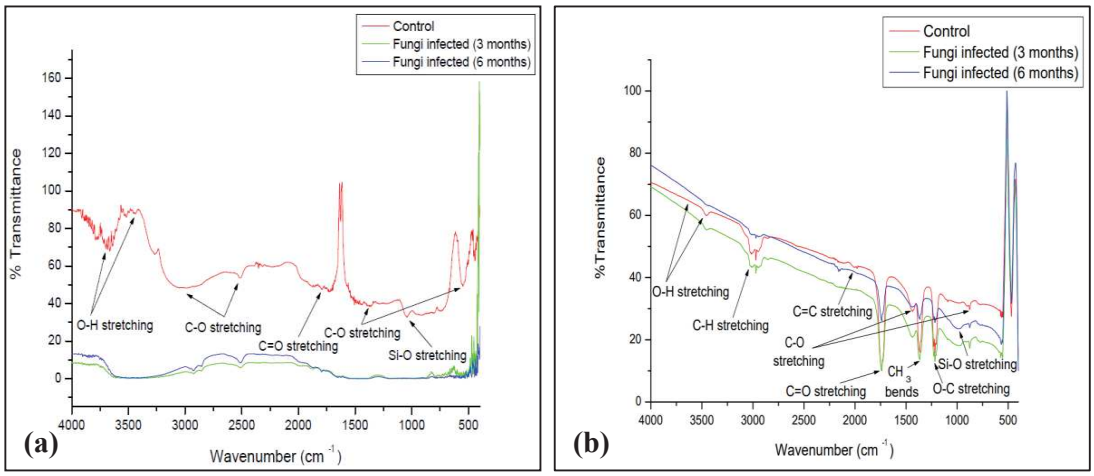


**Fig. 14** Mid-infrared spectra of control and *A. tamarii* infected: (a) M20 grade; (b) M40 grade concrete in the range 4000-400 $cm^{-1}$.

The control sample showed an envelope-shaped medium with symmetric band of 3450 $cm^{-1}$ attributable to O-H, which after 3 and 6 months of incubation became weak and very weak for M40 grade concrete and ultimately totally absent in M20 grade concrete. This O-H band can be misleading because the sample has absorbed water. Hydrogen bonding might alter the band shape and position. A weak asymmetric stretching band (Si-O) from C-S-H of the quartz (crystalline silica) was evident from 980 $cm^{-1}$ to 1000 $cm^{-1}$, that result extremely weak in high graded concrete [Fig. 14(b)] and totally disappearing in low graded concrete [Fig. 14(a)] after 3 and 6 months biodeterioration study. The shift in the Si-O band seen in the present study is comparable with the research work of Wiktor et al., (2011) in which Si-O polymerized to orthosilicate units ($SiO_4^{4-}$) at the time of weathering process.

### 2.2.6 Microscopic observation

#### 2.2.6.1 Scanning electron microscopy

After one month of fungal inoculation, the growth of the fungal biofilm was visible [Fig. 15(a)]. The surface biofilms on the stones frequently contain fungi, to use organic substrates like carbon, hydrogen and energy sources (Nuhoglu et al., 2006). Fungal spore and hyphae had been noticed on the exterior surface of the concrete cube at this point. When the samples had been inoculated for six months, the surface phenomenon undergone changed [Fig. 15(b)]. The spore in numbers was increased followed by growing fungal hyphae on the surface penetrated into the concrete materials. The development of calcium oxalate crystals [Fig.

15(c)] in samples that had been inoculated for six months further corroborate the effects of *A. tamarii*. Micro cracks were also seen on the concrete sample used in the present study [Fig. 15(d)], which could represent a pathway for the growth of surface fungus inside building materials.

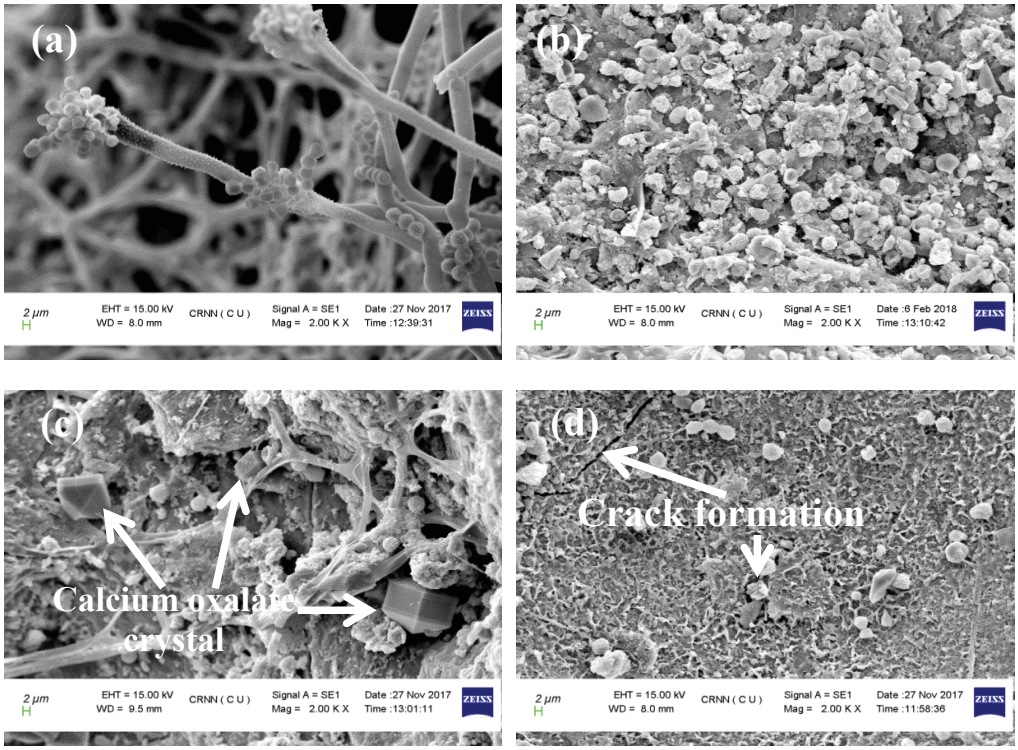


**Fig. 15** SEM images of *A. tamarii* infected concrete samples: a) 1 month; b) 6 month; c) calcium oxalate crystal formation; d) crack formation.

### 2.2.6.2 Stereo zoom microscopy

Compared to the control, the colour of the concrete cube was found to change to yellowish grey (5Y 8/1) according to a geological rock-color chart (Munsell 2009). The six-month-old contaminated concrete cubes displayed a phenomenon of disruption and missing concrete granules instead of a color change (Fig. 16). The pigmentation of *A. tamarii*, which may be metabolic products like melanin or by-products of other extracellular polymerization, is one of the prime reasons for color change of the concrete cube (Krumbein 1992). In the present investigation, corrosion was extensively studied in many folds and results indicated that the concrete surface is corroded by organic acids as produced by *A. tamarii.*

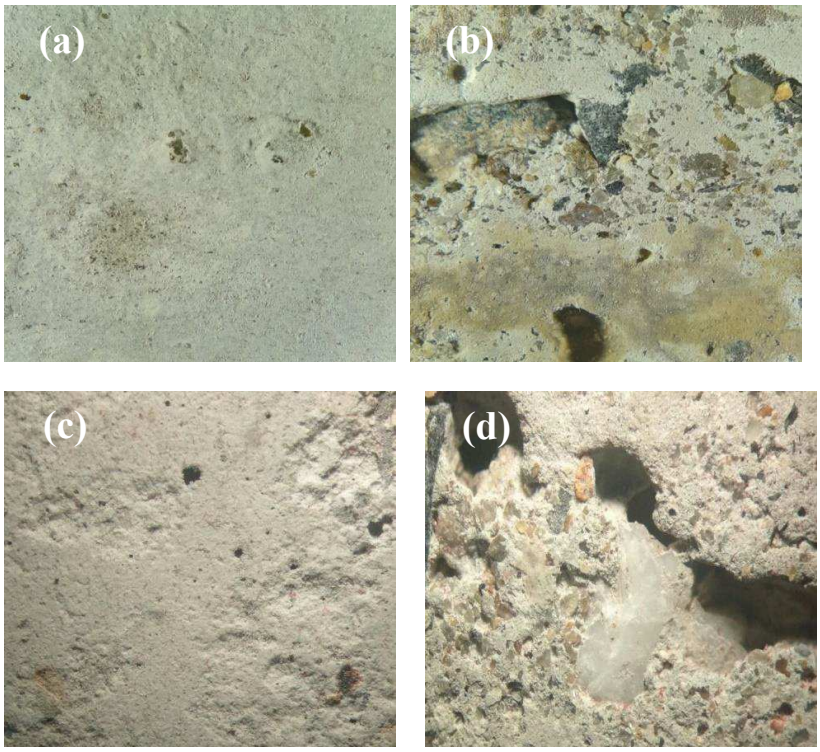


**Fig. 16** Stereo Microscopic images (1× magnification) of: a) control M20 grade; b) *A. tamarii* infected M20 grade; c) control M40 grade; d) *A. tamarii* infected M40 grade concrete cube surface after 6 months of incubation period.

### 2.3 Radiation dose selection study

#### 2.3.1 Radiosensitivity of *A. tamarii*

The sensitivity of the isolated fungus to UVC and gamma irradiation was evaluated with the help of Czapek Dox agar plate. Irradiated with different doses of ultraviolet and gamma radiation, the colony diameter (n = 3) were measured and compared to the diameter (n = 3) of the non-irradiated control after 7 days incubation period and exhibited in Fig. 17 and Fig. 18.

*A. tamarii* was resistant to ultraviolet exposure after 5, 10, and 15 mins, but was inactivated after 20 mins (Fig. 17). The colonies, which had a mean diameter of 2.0 ± 0.05 cm, were initially rendered inactive by the dose of 5 and 10 mins of exposure. Subsequently following a 1 day of incubation, the resistant cells began to grow once more and the colony continued to expand, eventually reaching diameters of 2.4 ± 0.01 and 2.3 ± 0.02 cm after 7 days, while the control colonies had 3.2 ± 0.03 cm diameters after the same incubation period (Fig. 17). However for 20 mins UVC, the diameter of the colony remained same after different

exposure intervals which were shown in Fig. 22. UVC light (250 µW/cm$^2$) killed most of the *Candida* organisms within 5 min as reported by Ishida et al., (1991).

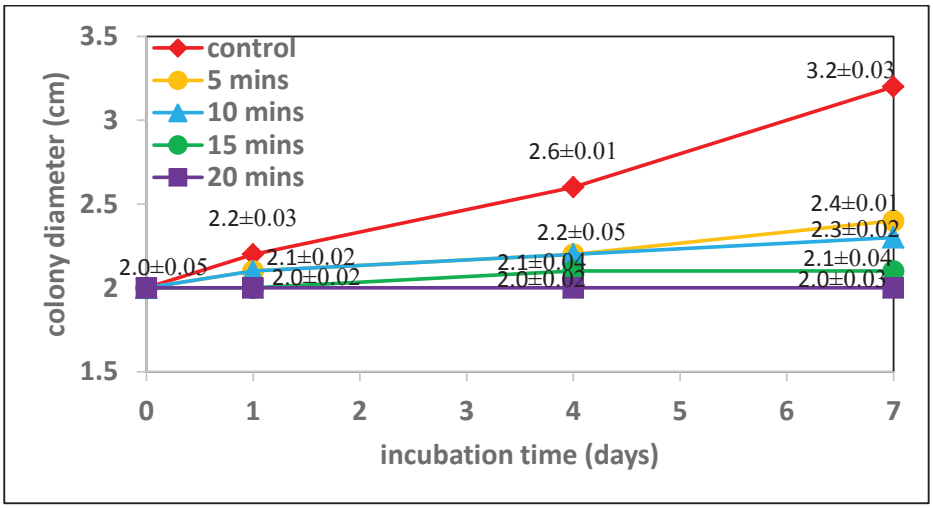


**Fig. 17** Responses of *A.tamarii* to UVC rays with doses of 5, 10, 15 and 20 mins in accordance to colony diameter (n = 3) during 7-days incubation.

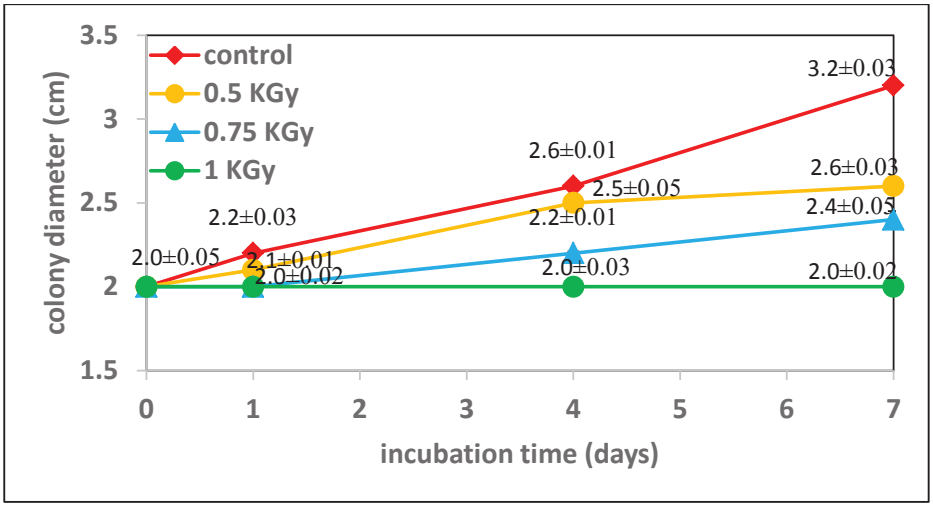


**Fig. 18** Responses of *A.tamarii* to gamma rays with doses of 0.5, 0.75 and 1 KGy in accordance to colony diameter (n = 3) during 7-days incubation.

The diameter of the gamma irradiated (0.5, 0.75 and 1 KGy) fungal colonies after 7 days of incubation were found to be 2.6 ± 0.03, 2.4 ± 0.05 and 2.0 ± 0.02 cm respectively (Fig. 18). However, it was shown in the plot that in case of gamma radiation with the doses of 0.5 and 0.75 KGy, the growth of *A. tamarii* slowed down compared to the control and finally totally inactive only at a dose equal to or above 1 KGy (Fig. 18). Similar kind of figure was obtained after application of gamma radiation where 1 KGy is the optimum dose for complete

inactivation of *A. tamarii*. Also, it was noted that *Trichoderma* sp. and *Aspergillus* sp. were inhibited at levels of 2 and 3 KGy, respectively, but *Curvularia* sp. and *Alternaria* sp. were only inhibited at 2.5 KGy (Maity et al., 2008). Based on the findings of the radiosensitivity of *A. tamarii* in our study, it was decided to use UVC and gamma radiation to treat the concrete cube.

### 2.3.2 Radiation on concrete cubes

#### 2.3.2.1 Weight variation

The weight reductions were calculated 30 days after exposure, and for control (non-infected and non-irradiated) samples, negligible weight reduction was noticed. After the surface precipitates were cleared away, *A. tamarii* inoculated i.e. biodeteriorated concrete cubes revealed a weight reduction of 0.56 ± 0.01%.

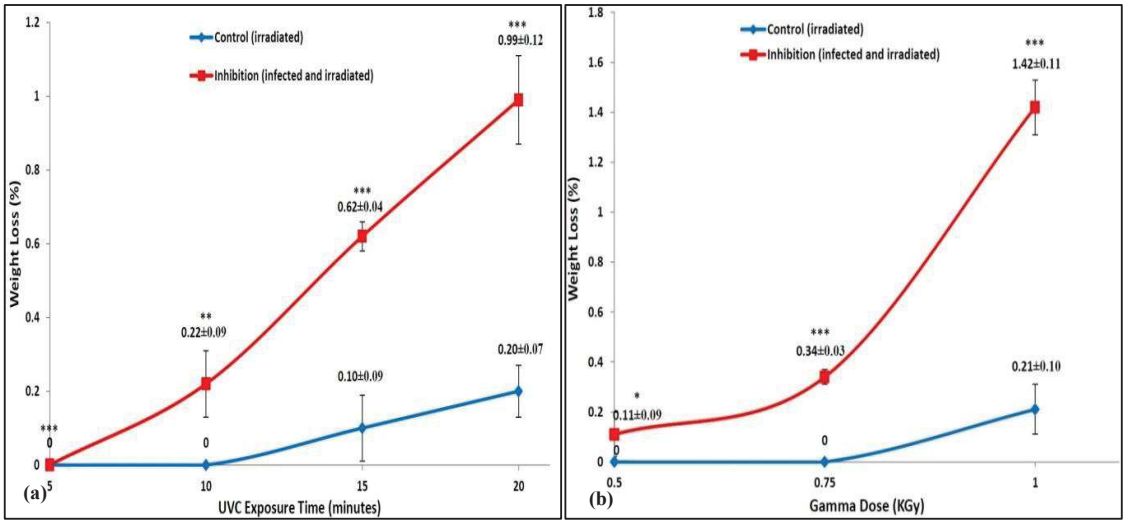


**Fig. 19** Weight reduction in percentage for: a) ultraviolet; b) gamma radiated cube samples (n =3) after a month.

Inhibition cube samples showed very marginal reduction of weight after exposed to UV rays for 5 min. After exposed to ultraviolet radiation for 10, 15 and 20 min, the cube samples showed 0.22 ± 0.09%, 0.62 ± 0.01% and 0.99 ± 0.12% weight reduction respectively [Fig. 19(a)], while inhibition cubes lost 0.11 ± 0.09%, 0.34 ± 0.01%, 1.42 ± 0.11% of their weight after being exposed to gamma radiation for 0.5, 0.75 and 1 KGy [Fig. 19(b)]. It is interesting to note that variations of concrete weight were also observed for irradiated control cube samples that were run in sterile Czapek Dox medium i.e. negligible after 5 and 10 min UV

ray, 0.10 ± 0.09% and 0.20 ± 0.07% after 15 and 20 min UV ray, negligible after 0.5 and 0.75 KGy gamma ray and 0.21 ± 0.10% after 1 KGy gamma exposure (Fig. 19). In addition, it was also observed that weight losses of inhibition cubes that had been infected and exposed to radiation were higher ($p < 0.05$, $p < 0.01$ and $p < 0.001$) than those of control samples (irradiated). The loss of weight for the inhibition samples was found less with respect to a gamma dose of 0.5 KGy compared to 0.75 and 1 KGy respectively as shown in [Fig. 19(b)].

The loss of weight for inhibited samples was caused by fungus as well as irradiation, whereas for control samples weight loss occurred only due to radiation. However, based on weight losses, radiation damage for a concrete was clearly observed after infected cube was exposed to radiation (inhibition) at a dosage of 1 KGy [Fig. 19(b)] in contrast to samples that had biodeteriorated. Cement materials lose weight throughout the irradiation process, which is likely due to the loss of chemically bound, physically bound, and unbound water. Additionally, present research showed that concrete cubes lost greater weight at higher temperatures or radiation doses (Fig. 19). The loss of weight of concrete cube was an indication that it was becoming dehydrated as a result of the increase in radiation doses.

#### 2.3.2.2 Compressive strength variation

The average compressive strength for control (non-infected and non-irradiated) and fungal-infected (biodeterioration) 30-day-old cubes were 19.74 ± 0.46 and 18.88 ± 0.43 $N/mm^2$ respectively (Fig. 20). These findings demonstrated that compared to the control (non-infected and non-irradiated), *A. tamarii* infection accelerated the process of deterioration, lowering ($p < 0.05$) the compressive strength of the concrete cubes.

The lowest ($p < 0.001$) compressive strength 17.84 ± 0.28 $N/mm^2$ was found in UVC-irradiated infected (inhibition) concrete cubes after 20 min of exposure [Fig. 20(a)], followed by samples exposed for 5, 10, and 15 min (20.20 ± 0.34, 19.26 ± 0.26 and 18.46 ± 0.34 $N/mm^2$). The compressive strength of infected cubes after undergoing 5 and 10 min of ultraviolet ray (inhibition) showed higher strength [Fig. 20(a)] in comparison to *A.tamarii* infected (biodeteriorated) cubes. The most dangerous waveband, UVC, probably destroy both *A. tamarii* conidia and spores.

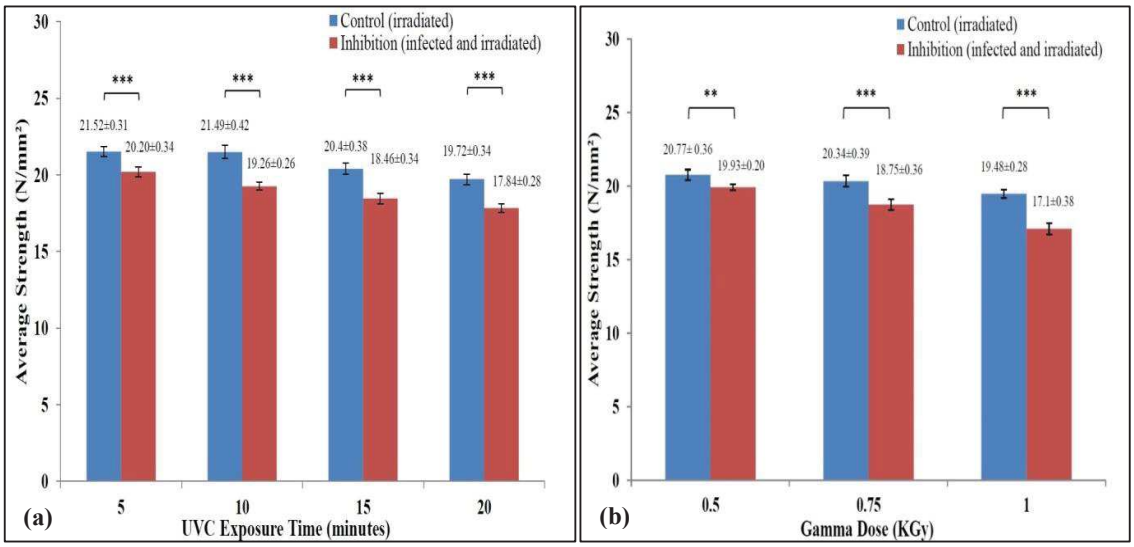


**Fig. 20** Compressive strength (N/mm$^2$) variation for: a) ultraviolet; b) gamma irradiated cube samples (n = 3) after a month.

Similarly gamma irradiation with a dose of 0.5 KGy reducing ($p < 0.01$) compressive strength from 20.77 ± 0.36 N/mm$^2$ (control) to 19.93 ± 0.20 N/mm$^2$ (inhibition), whereas 19.48 ± 0.28 N/mm$^2$ (control) to 17.10 ± 0.38 N/mm$^2$ (inhibition) strength loss ($p < 0.001$) had been also observed after irradiating the cube with 1 KGy dose of gamma radiation [Fig. 20(b)]. Craeye et al., (2015) found that samples aged for a longer period of time prior to irradiation at high dose rates (1.36 KGy/h) showed a larger decrease in compressive strength. Low dosage rates did not show this impact. Loss of compressive strength is also correlated with water hydration in the cement plus pore water radiolysis or pore water evaporation under radiation heat. The cement's hydration level and strength were decreased during irradiation due to a loss of oxygen and hydrogen radiolytic species (Soo and Milian 2001).

### 2.3.2.3 Variation in elemental composition

The calcium percentage in the infected concrete (49.88 ± 0.65%) was lower ($p < 0.001$) than control sample (72.32 ± 0.21%) because *A. tamarii* assisted in the leaching of calcium ions from the concrete cube (Fig. 21). Additionally, this phenomenon has been discussed in some other studies as reported in the literature (Sanchez-Silva and Rosowsky 2008; Gu et al., 1998). Simultaneously, as the amount of calcium leaching was reduced, the percentage of silica was found to be decreased.

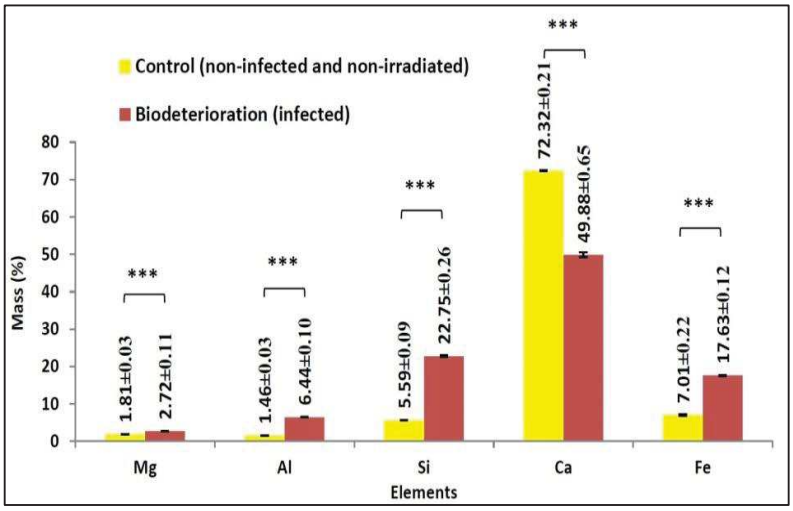


**Fig. 21** Mass fraction (%) of major elements for control and biodeteriorated samples (n = 3) after a month.

Infected concrete as exposed to UV radiation (inhibition) for 5, 10, 15, and 20 minutes had mass percentages of calcium of 75.75 ± 0.16%, 69.12 ± 0.22%, 48.54 ± 0.17%, and 36.54 ± 0.27%, respectively [Fig. 22(a)]. Samples exposed to UVC radiation for 15 and 20 mins (inhibition) showed greater calcium losses than samples exposed to 5 and 10 mins UVC radiation. However, compared to the control (irradiated) samples, the mass % of calcium was around the same for the 5 and 10 min irradiated infected (inhibition) samples and statistically significant [Fig. 22(a)]. Another finding from the EDXRF analysis was that the calcium concentration of infected cubes following exposure to 5 and 10 minutes of UVC radiation (inhibition) exhibited greater calcium content compared to only infected i.e. biodeteriorated cubes [Fig. 21 and Fig. 22(a)]. The results of the present investigation thus revealed that the exposure to ultraviolet light for 5 and 10 mins had been beneficial for reducing calcium leaching from concrete and preventing fungal biodeterioration of concrete.

In a bar graph [Fig. 22(b)], the mass (%) and elemental composition of various concrete elements are shown. When compared to calcium percentage (70.95 ± 0.30%) of concrete samples after exposed to 0.5 KGy doses of gamma radiation (inhibition), the percentages of calcium (56.53 ± 0.19% and 57.29 ± 0.15%) were decreased after the application of 0.75 and 1 KGy gamma doses [Fig. 22(b)]. In fact the production of the very insoluble phase $CaO_2.8H_2O$, which results in the eradication of ettringite and portlandite, is mainly due to the dropping of calcium percentage in concrete exposed to large doses of gamma radiation

(Bouniol and Aspart 1998). With the increase in radiation doses, the mass (%) of additional trace elements like silica, iron, and aluminium also increased (Fig. 22).

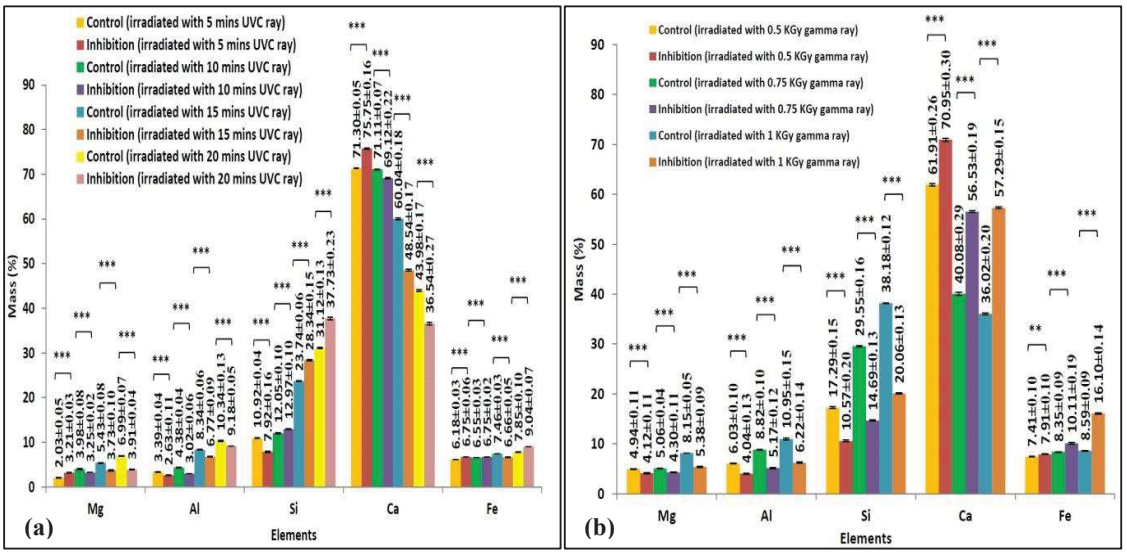


**Fig. 22** Mass fraction (%) of major elements for: a) UVC; b) gamma irradiated control and inhibition samples (n = 3) after a month.

### 2.3.2.4 Changes in functional groups

All concrete samples' infrared spectra at 3640 $cm^{-1}$ revealed portlandite's hydroxyl vibrations. Portlandite [$Ca(OH)_2$] was transformed during the carbonation and leaching process. Concrete samples (control and inhibition) which were exposed to ultraviolet ray for 5 mins peaked at 1400, 874 and 705 $cm^{-1}$ respectively and displayed a prominent symmetrical stretching band (C-O) of calcium carbonate. After being exposed to ultraviolet radiation for 10, 15, and 20 mins respectively, the C-O absorption band became medium and weak (Fig. 23). In IR spectra obtained from irradiated concrete samples earlier, Nagabhushana et al. (2008) also observed such band behaviour, which showed a shift towards lower wavenumbers and a decrease in the intensity of the calcite (1350, 874, and 712 $cm^{-1}$) stretching modes. The deformation and fracture of the carbonate groups found in calcite, as well as greater radiation dosages and fungus, have all been linked to this alteration in IR spectra. All of the concrete samples showed an envelope-shaped strong and broad symmetrical band (O-H) of water at 3450 $cm^{-1}$. The decrease in intensity of the broad band at 3400 $cm^{-1}$ (Fig. 23 and Fig. 24) in biodeterioration and inhibition (except lower radiation dose) samples compared to both control (non-infected and non-irradiated as well as only irradiated) demonstrated the clear indication of the decrease in $H_2O$ content.

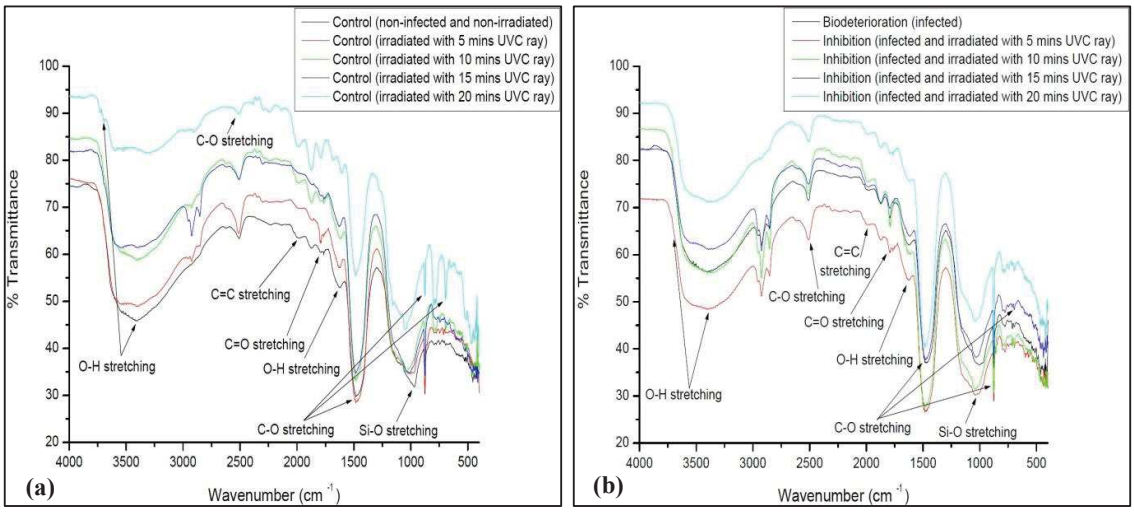


**Fig. 23** FTIR transmittance spectrum of: a) control concrete (non-irradiated and UVC irradiated); b) biodeterioration concrete and inhibition concrete (UVC irradiated) samples after a month.

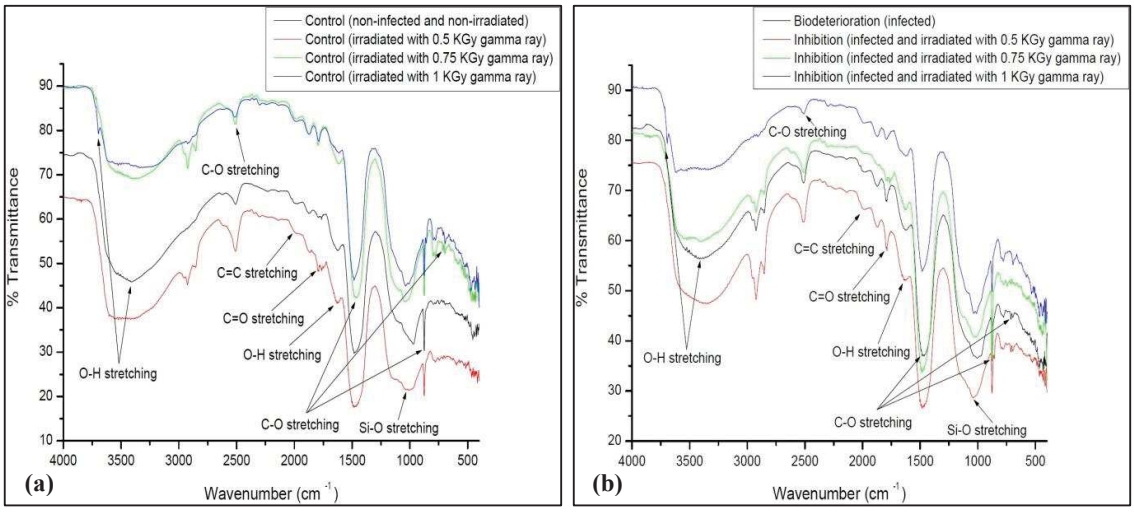


**Fig. 24** FTIR transmittance spectrum of: a) control concrete (non-infected and gamma irradiated); b) biodeterioration concrete and inhibition concrete (gamma irradiated) samples after a month.

After receiving a high dose of radiation, another asymmetrically stretching strong band (980 $cm^{-1}$) from the C-S-H of the crystalline silica mineral quartz (Si-O) became medium that was both for control (irradiated) and inhibition concrete samples (Fig. 23 and Fig. 24). Si-O is typically a covalent chemical bond. Consequently, gamma radiation could degrade materials made of silica. In the mid-IR region of the studied concrete samples, the major bands observed include carbonate, silicate, and water. After 30 days of incubation, these bands in

the fungi-affected (biodeteriorated) concrete became medium and thereafter weakened compared to the non-infected and non-irradiated concrete sample (Fig. 23 and Fig. 24). These bands were found weaker after 180 days of exposure and were eventually be broken by fungus. The bands also weakened as a result of radiation damage when control and inhibition samples were exposed to 0.75 and 1 KGy doses of gamma radiation (Fig. 24). However, the band was stronger after 0.5 KGy dose of gamma irradiation in the irradiated (control and inhibition) concrete sample than the infected (biodeteriorated) concrete sample (Fig. 24).

### 2.4 Inhibition of biodeterioration with selected radiation dose

#### 2.4.1 Characterisation of concrete cubes

##### 2.4.1.1 Weight variation

The weight loss percentage in UVC irradiated infected concrete cubes (0.28 ± 0.09%) was observed to be the lowest after 180 days incubation period followed by gamma irradiated infected (0.72 ± 0.08%) and non-irradiated infected (2.22 ± 0.04%) cubes (Fig. 25). Additionally, when the concrete cube was kept in fungal medium, it shows almost negligible weight loss (0.85 ± 0.02%) over time.

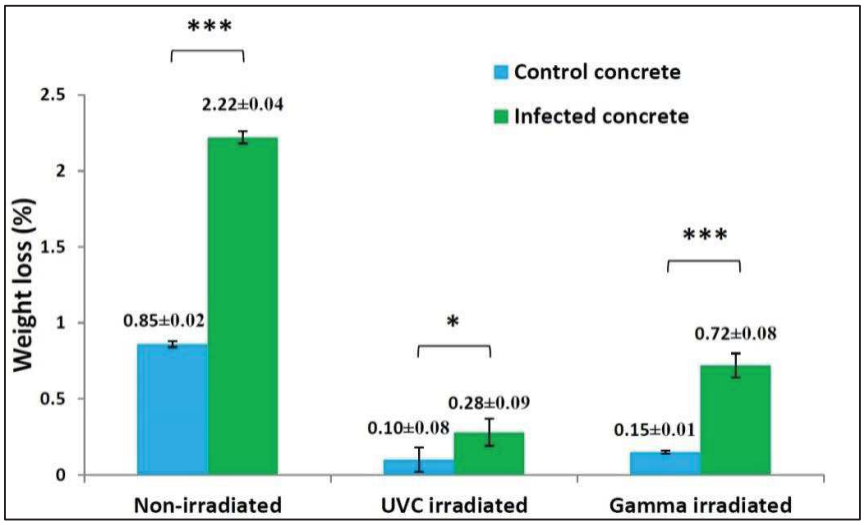


**Fig. 25** Weight loss of non-irradiated, ultraviolet and gamma irradiated concrete cubes (n = 3) after 6 months.

Also some weight losses that observed for UVC (0.28 ± 0.09%) and gamma (0.72 ± 0.08%) irradiated cubes (Fig. 25) because from radiosensitivity study complete depletion of *A. tamarii* was not observed with chosen radiation dose (Fig. 17 and Fig. 18) without affecting

weight properties of concrete due to radiation damage (Fig. 19). After irradiation, the colony of *A. tamarii* was still found to persist and being deteriorated the concrete cubes. However, complete inhibition of fungal population and losses weight of concrete cubes were observed even when samples were irradiated with higher doses of radiation.

### 2.4.1.2 Compressive strength variation

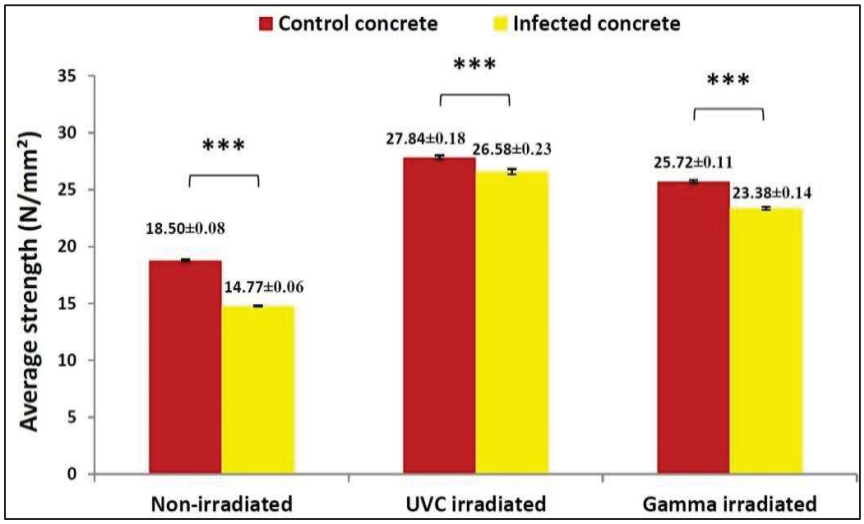


**Fig. 26** Compressive strength loss ($N/mm^2$) of non-irradiated, ultraviolet and gamma irradiated concrete cubes (n = 3) after 6 months.

The compressive strength of non-irradiated control and infected cubes after 6 months were 18.50 ± 0.08 and 14.77 ± 0.06 $N/mm^2$ respectively (Fig. 26). Moreover, our present investigation agreed with the results of some other researcher's reports on concrete cube as referred below, which revealed that due to fungal infection compressive strength of concrete have been decreased with time (Yakovleva et al., 2018). For the irradiated control samples, where Czapek Dox medium was added initially after irradiated and fungal activity was found absent, the increment of compressive strength (27.84 ± 0.18 and 25.72 ± 0.11 $N/mm^2$) were observed compared to the non-irradiated control samples (18.50 ± 0.08 $N/mm^2$). Significant increase in compressive strength was also observed for UVC (26.58 ± 0.23 $N/mm^2$) and gamma (23.38 ± 0.14 $N/mm^2$) radiated infected concrete cubes compared to the non-irradiated infected samples (14.77 ± 0.06 $N/mm^2$) after 180 days of incubation (Fig. 26). In contrast to the findings of Rezaei-Ochbelagh et al., (2010) present experimental findings demonstrate that compressive strength of radiated concrete cube has been improved due to gamma effect.

### 2.4.1.3 Variation in elemental composition

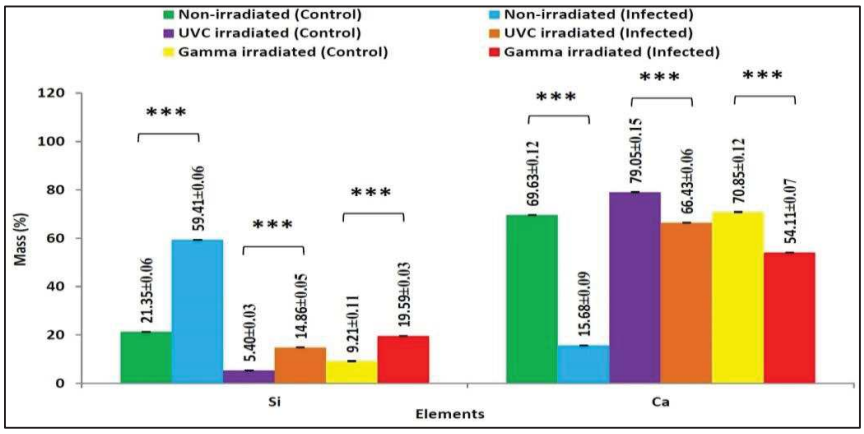


**Fig. 27** Mass fraction of silicon and calcium of non-irradiated and irradiated concrete samples (n = 3) after 6 months.

The calcium content of the non-irradiated infected cubes was found to be decreased ($p < 0.001$) compared to non-irradiated control ones because *A. tamarii* helps to leach calcium from concrete cube as discussed in previous study. But the mass percentage of calcium was found to be increased in UVC and gamma irradiated (infected) concrete whereas the mass percentage of silicon was decreased as compared to the non-irradiated (infected) sample (Fig. 27). Hence the chosen ultraviolet and gamma radiation dose were effective to decrease the leaching rate of calcium from the concrete cube. Consequently, the decrease in silicon concentration leads to an increase in calcium concentration. The chemical composition of all elements of concrete cubes must always add up to 100%.

### 2.4.1.4 Variation in functional groups

Wide stretched bands centred around 3650 $cm^{-1}$ represents the hydroxyl groups (OH) of the portlandite [$Ca(OH)_2$]. This band was subsequently broken and faded completely after 6 months in *A. tamarii* infected (non-irradiated) samples. After irradiation, this stretching band in the infected sample became strong or remains unchanged (Fig. 28). The sharp and strong C-O stretches in all the control IR spectrum at 1400, 874 and 611 $cm^{-1}$ indicate the presence of calcite ($CaCO_3$). Similar strong peaks can be observed in the IR spectra of the UVC and gamma irradiated infected cubes after 6 months. Additionally this band can be seen to gradually flatten after six months in *A. tamarii* infected (non-irradiated) sample [Fig. 28(b)]. At 980 $cm^{-1}$ to 1000 $cm^{-1}$, a weak asymmetric stretching band (Si-O) of the crystalline silica material quartz was seen in irradiated (control and infected) specimens, but it completely

disappeared after the fungal deterioration (infected and non-irradiated) (Fig. 28). It shows that the chosen dose of UVC and gamma radiation helps the depletion of fungal population, thereby improves the chemical properties of concrete.

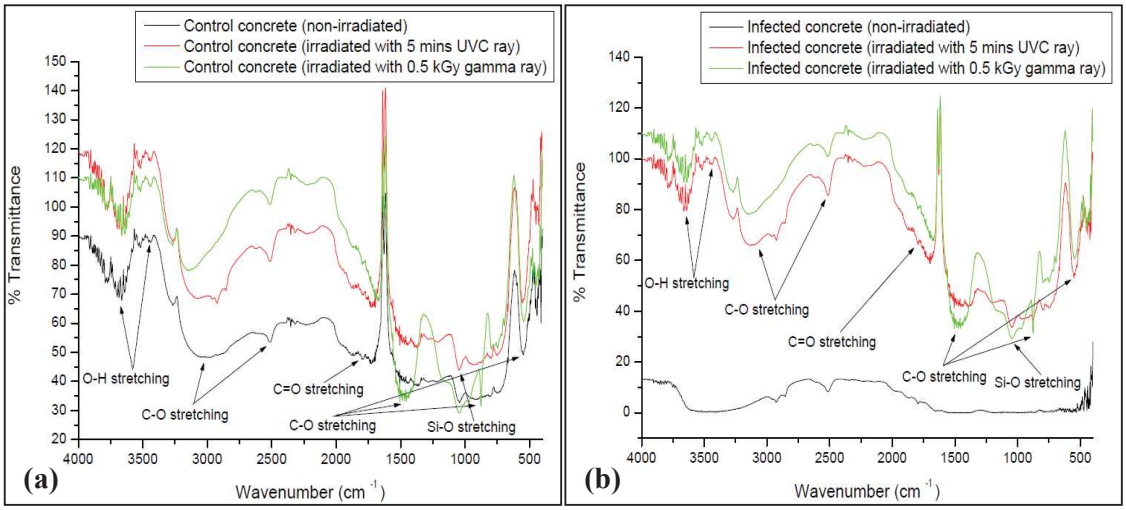


**Fig. 28** Mid-infrared spectra of: a) control; b) infected concrete samples after 6 months.

### 2.4.1.5 Stereo zoom microscopic observation

The stereomicroscopic images showed that after irradiation *A. tamarii* infected concrete cube surface remains same as compared to the irradiated control samples. Also no cavities were formed in UVC and gamma radiated infected cube surface (Fig. 29 and Fig. 30) compared to the only *A. tamarii* infected samples (Fig. 16). But the color of irradiated as well as infected cube surface becomes yellowish, which is probably due to production of fungal metabolic pigments melanin on the concrete surface.

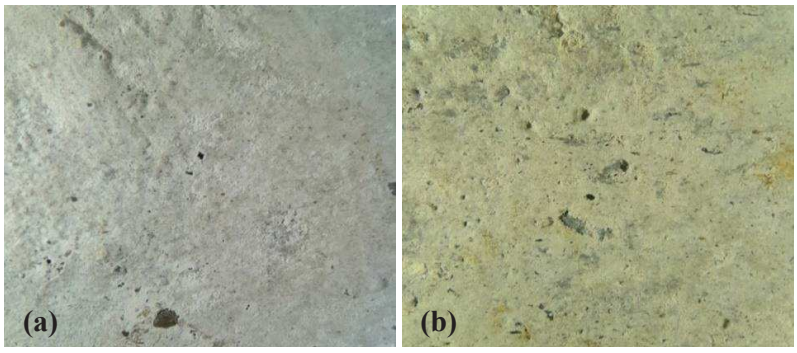


**Fig. 29** Stereo microscopic images (1× magnification) of UVC irradiated: a) control; b) *A. tamarii* infected concrete cube surface after 6 months.

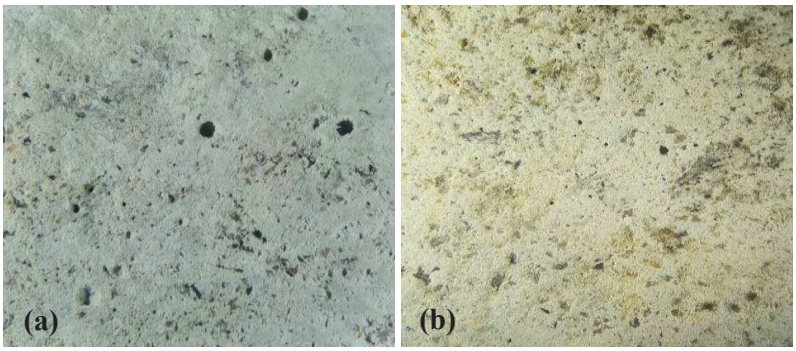


**Fig. 30** Stereo microscopic images (1× magnification) of gamma irradiated: a) control; b) *A. tamarii* infected concrete cube surface after 6 months.

### 2.4.2 *In situ* model for conservation of heritage building

Based on the findings of this study, an *in situ* model for conservation effect of heritage buildings made of concrete is recommended (Fig. 31). According to this model, five UVC lights will be installed (4 side wall lights and 1 upper wall light) with an intensity of 625 µw/cm$^2$ and a peak wavelength of 254 nm at a distance of 15 cm from the walls. Another option will to place radioactive material that releases gamma rays in a properly constructed collimator inside the room.

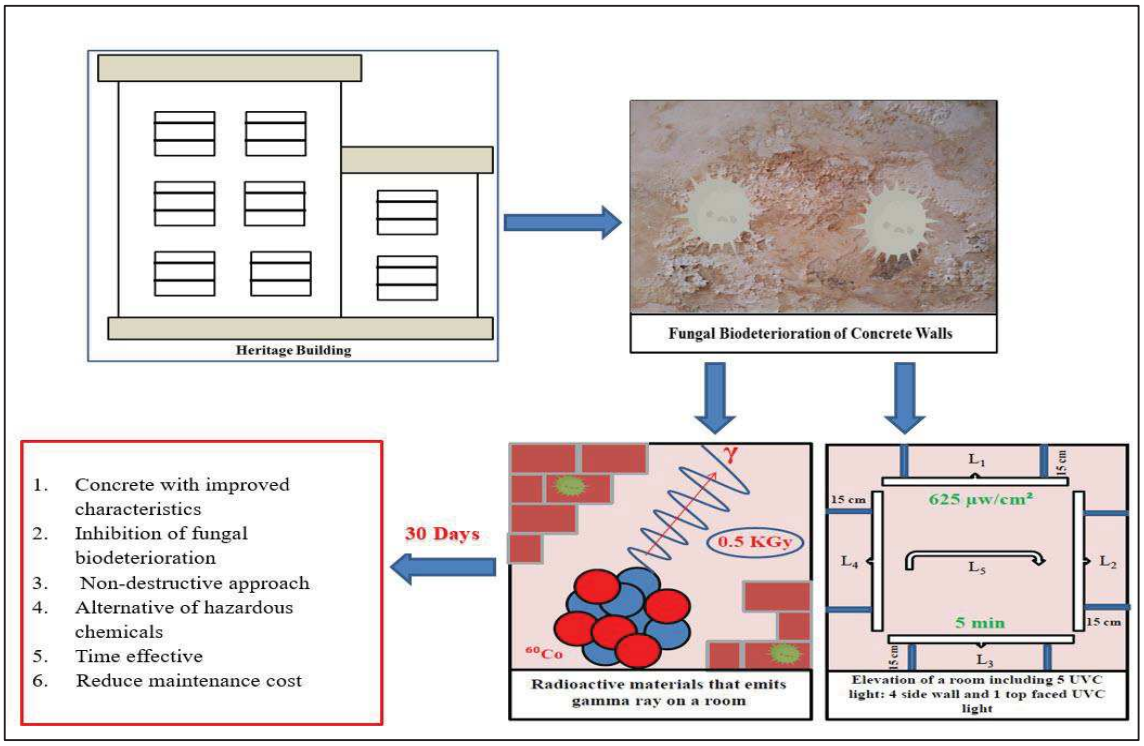


**Fig. 31** *In situ* model for preventing fungal biodeterioration of historic building.

The duration of the UV exposure shall be 5 mins, whereas 0.5 KGy dose of gamma radiation needed to prevent the growth of mould on concrete walls at least twice a year. The concrete walls will be better and fungal-free as a consequence, which save time and money and being non-destructive.

## Conclusions

An assessment of the airborne fungi in the indoor environment was experimentally investigated in the present study. The results of air sampling revealed that the highest percentage of culturable airborne fungi was *Aspergillus* sp. followed by *Penicillium* sp. So, the present study confirmed that *Aspergillus* sp. was the most dominant airborne fungus in indoor environment. The weight loss (%) and calcium release of concrete piece, organic acid analysis of fungal medium indicated that *Aspergillus tamarii* imparted maximum loss as compared to *Aspergillus niger*, *Aspergillus flavus* and *Penicillium oxalicum*. The SEM images displayed fungal colonization, ettringite and crack formation on *A. tamarii* infected concrete surface which also supports the present phenomenon and decision was taken to precede further work *A. tamarii* only. From six month biodeterioration study, the evidential examination suggested that isolated fungi *A. tamarii* enhance the deterioration phenomena of M40 and M20 graded concrete in different ways and also impose changes in their physical, mechanical, chemical and aesthetic properties that leads to decrease in the lifespan of concrete structure. In addition, deterioration of M20 grade concrete was more compared to M40 grade concrete.

The radiosensitivity of the isolated fungus had been suggested that fungal population depletion was observed after application of different doses of radiation on the contrary complete inhibition of *A. tamarii* would have been noticed after 20 mins UVC exposure and 1 KGy dose of gamma radiation. The present study also reveals that after 30 days 5 mins UVC and 0.5 KGy gamma radiation dose inhibit the loss of physical, mechanical and chemical properties of concrete due to fungus. Hence, 5 min UVC exposure and 0.5 KGy doses of gamma radiation for inhibition of fungal biodeterioration of concrete had been selected for further study. The present experimental investigations (inhibition study) suggest that chosen doses of radiation delayed the fungal growth without affecting concrete properties after 180 days compared to the control.

## Future scope of work

The following activities can be performed in near future for further investigations on inhibition of fungal biodeterioration of concrete.

- In order to more clearly explain the efficiency of radiation, it is also advised that biodeterioration as well as inhibition with radiation of fungal biodeterioration of concrete can be expanded for extended periods of time.
- The scope of future research work can be widened using the technique *in situ* on actual colonized concrete-based buildings.

## References


Aldosari, M. A., Darwish, S. S., Adam, M. A., Elmarzugi, N. A., & Ahmed, S. M. (2019). Using ZnO nanoparticles in fungal inhibition and self-protection of exposed marble columns in historic sites. Archaeological and Anthropological Sciences, 11, 3407-3422.

Allsopp, D. (2011). Worldwide wastage: the economics of biodeterioration. Microbiol Tod, 38(4), 150-153.

Amann, R. I., Krumholz, L., & Stahl, D. A. (1990). Fluorescent-oligonucleotide probing of whole cells for determinative, phylogenetic, and environmental studies in microbiology. Journal of bacteriology, 172(2), 762-770.

Aquino, R. S. S., Silveira, S. S., Pessoa, W. F. B., Rodrigues, A., Andrioli, J. L., Delabie, J. H. C., & Fontana, R. (2013). Filamentous fungi vectored by ants (Hymenoptera: Formicidae) in a public hospital in north-eastern Brazil. Journal of Hospital Infection, 83(3), 200-204.

Bertrand, L., Schöder, S., Joosten, I., Webb, S. M., Thoury, M., Calligaro, T., Anheim, E., & Simon, A. (2023). Practical advances towards safer analysis of heritage samples and objects. TrAC Trends in Analytical Chemistry, 117078.

Borderie, F., Alaoui-Sehmer, L., Bousta, F., Orial, G., Rieffel, D., Richard, H., & Alaoui-Sosse, B. (2012). UV irradiation as an alternative to chemical treatments: a new approach against algal biofilms proliferation contaminating building facades, historical monuments and touristic subterranean environments. Algae: ecology, economic uses and environmental impact. Nova Science Publishers, Inc. Hauppauge, New York, 1-28.

Bouniol, P., & Aspart, A. (1998). Disappearance of oxygen in concrete under irradiation: the role of peroxides in radiolysis. Cement and concrete research, 28(11), 1669-1681.

Craeye, B., De Schutter, G., Vuye, C., & Gerardy, I. (2015). Cement-waste interactions: Hardening self-compacting mortar exposed to gamma radiation. Progress in Nuclear Energy, 83, 212-219.

Gu, J. D., Ford, T. E., Berke, N. S., & Mitchell, R. (1998). Biodeterioration of concrete by the fungus Fusarium. International biodeterioration & biodegradation, 41(2), 101-109.

Hanehara, S., & Oyamada, T. (2010). Reproduction of delayed ettringite formation (DEF) in concrete and relationship between DEF and alkali silica reaction. Monitoring and Retrofitting of Concrete Structures-BH Oh, et al.(eds), Korea Concrete Institute, Seoul.

Ishida, H., Nahara, Y., Tamamoto, M., & Hamada, T. (1991). The fungicidal effect of ultraviolet light on impression materials. The Journal of Prosthetic Dentistry, 65(4), 532-535.

Kontani, O., Ichikawa, Y., Ishizawa, A., Takizawa, M., & Sato, O. (2014). Irradiation effects on concrete structures. Infrastructure systems for nuclear energy, 459-473.

Krumbein, W. E. (1992, May). Colour changes of building stones and their direct and indirect biological causes. In Proceedings of the 7th International Congress on Deterioration and Conservation of Stone: held in Lisbon, Portugal, 15-18 June 1992 (pp. 443-452).

Liaud, N., Ginies, C., Navarro, D., Fabre, N., Crapart, S., Gimbert, I. H., Levasseur, A., Raouche, S., & Sigoillot, J. C. (2014). Exploring fungal biodiversity: organic acid production by 66 strains of filamentous fungi. Fungal Biology and Biotechnology, 1(1), 1-10.

Maity, J. P., Chakraborty, A., Chanda, S., & Santra, S. C. (2008). Effect of gamma radiation on growth and survival of common seed-borne fungi in India. Radiation Physics and Chemistry, 77(7), 907-912.

Munsell, A. H. (2009). Geological Rock-Color Chart, Produced by Munsell Color.

Nagabhushana, H., Prashantha, S. C., Nagabhushana, B. M., Lakshminarasappa, B. N., & Singh, F. (2008). Damage creation in swift heavy ion-irradiated calcite single crystals: Raman and Infrared study. Spectrochimica Acta Part A: Molecular and Biomolecular Spectroscopy, 71(3), 1070-1073.

Nevalainen, A., Täubel, M., & Hyvärinen, A. (2015). Indoor fungi: companions and contaminants. Indoor air, 25(2), 125-156.

Nuhoglu, Y., Oguz, E., Uslu, H., Ozbek, A., Ipekoglu, B., Ocak, I., & Hasenekoglu, I. (2006). The accelerating effects of the microorganisms on biodeterioration of stone monuments under air pollution and continental-cold climatic conditions in Erzurum, Turkey. Science of the total environment, 364(1-3), 272-283.

Reddy, M. K., & Srinivas, T. (2017). Mold allergens in indoor play school environment. Energy Procedia, 109, 27-33.

Rezaei-Ochbelagh, D., Mosavinejad, H. G., Molaei, M., Azimkhani, S., & Khodadoost, M. (2010). Effect of low-dose gamma-radiation on concrete during solidification. International Journal of the Physical Sciences, 5(10), 1496-1500.

Rose, A. H. (1981). History and Scientific Basis of Microbial Biodeterioration of Materials. In" Microbial Biodeterioration" Economic Microbiology Vol. 6, (Rose, AH, Ed.).

Sanchez-Silva, M., & Rosowsky, D. V. (2008). Biodeterioration of construction materials: state of the art and future challenges. Journal of Materials in Civil Engineering, 20(5), 352-365.

Sarah, A. A., & Ee, A. G. R. (2017). Indoor and outdoor concentrations of bioaerosols and meteorological conditions of selected salons in four areas of Ibadan North local government area. Int J Environ Monit Anal, 5, 83.

Sarkhosh, M., Najafpoor, A. A., Alidadi, H., Shamsara, J., Amiri, H., Andrea, T., & Kariminejad, F. (2021). Indoor Air Quality associations with sick building syndrome: An application of decision tree technology. Building and Environment, 188, 107446.

Skora, J., Gutarowska, B., Pielech-Przybylska, K., Stępień, Ł., Pietrzak, K., Piotrowska, M., & Pietrowski, P. (2015). Assessment of microbiological contamination in the work environments of museums, archives and libraries. Aerobiologia, 31, 389-401.

Soo, P., & Milian, L. M. (2001). The effect of gamma radiation on the strength of Portland cement mortars. Journal of materials science letters, 20(14), 1345-1348.

Sykes, J. M. (1988). Sick building syndrome: a review. Health and Safety Executive, Technology Division.

Tong, G. S. (2018). Processes and Mechanisms Responsible for Microbial Degradation of the Chemical and Structural Integrity of Concrete. Imperial College London.

Wiktor, V., De Leo, F., Urzì, C., Guyonnet, R., Grosseau, P. H., & Garcia-Diaz, E. (2009). Accelerated laboratory test to study fungal biodeterioration of cementitious matrix. International Biodeterioration & Biodegradation, 63(8), 1061-1065.

Wiktor, V., Grosseau, P., Guyonnet, R., Garcia-Diaz, E., & Lors, C. (2011). Accelerated weathering of cementitious matrix for the development of an accelerated laboratory test of biodeterioration. Materials and structures, 44, 623-640.

Yakovleva, G., Sagadeev, E., Stroganov, V., Kozlova, O., Okunev, R., & Ilinskaya, O. (2018). Metabolic activity of micromycetes affecting urban concrete constructions. The Scientific world journal, 2018.

Yu, C., Wang, Y., Cao, H., Zhao, Y., Li, Z., Wang, H., Chen, M., & Tang, Q. (2020). Simultaneous determination of 13 organic acids in liquid culture media of edible fungi using high-performance liquid chromatography. BioMed Research International, 2020.

**Signature of Candidate with date:** Anirban Chaudhuri 18/12/2023

**Signature of Supervisors with date and official seal:**

18.12.2023

DR. S. N. MUKHERJEE
Professor
CIVIL ENGINEERING DEPT.
JADAVPUR UNIVERSITY
KOLKATA-700032, (W.B)

Subarna Bhattacharyya 18.12.23.

**Subarna Bhattacharyya, PhD**
**Assistant Professor**
**School of Environmental Studies**
**Jadavpur University**
**Kolkata 700032, INDIA**

Anindita Chakraborty 18.12.23

डॉ. अनिंदिता चक्रबोर्ती / Dr. Anindita Chakraborty
वैज्ञानिक-एच / Scientist-H
यूजीसी-डीएई कंसोर्टियम फॉर साइंटिफिक रिसर्च, कोलकाता केन्द्र
UGC-DAE Consortium for Scientific Research, Kolkata Centre
ब्लाक-एल.बी.-८ बिधाननगर / Block-LB-8, Bidhannagar
कोलकाता (प.बं.)-७०००९६ / Kolkata (W.B.)-700106